Mutations in Rv2983 as a novel determinant of resistance to nitroimidazole drugs in

Mycobacterium tuberculosis

Dalin Rifat[1], Si-Yang Li[1], Thomas Ioerger[2], Jean-Philippe Lanoix[3], Jin Lee[1], Ghader Bashiri[4],

James Sacchettini[5] and Eric Nuermberger[1,*]

[1] Center for Tuberculosis Research, Johns Hopkins University School of Medicine, 1550

Orleans Street, Baltimore, MD 21287, USA

[2] Department of Computer Science, Texas A&M University, College Station, TX, 77843, USA

[3] Department of Infectious Diseases, Amiens University Hospital, Amiens, France

[4] Laboratory of Structural Biology and Maurice Wilkins Center for Molecular Biodiscovery,

 School of Biological Sciences, University of Auckland, Auckland 1010, New Zealand

[5] Department of Biochemistry and Biophysics, Texas A&M University, College Station, TX,

 77843, USA

*Corresponding author. Email: enuermb@jhmi.edu   Tel: 410-502-7683

SIGNIFICANCE

Nitroimidazole pro-drugs represent a promising new class of anti-tuberculosis drugs. Reliable

methods to assure nitroimidazole susceptibility are critical to assure their optimal use. Yet, the

spectrum of nitroimidazole resistance mutations remains incompletely characterized. Using 161

pretomanid-resistant *Mycobacterium tuberculosis* isolates selected in pretomanid-treated mice,

we discovered a novel resistance determinant, *Rv2983*, required for cofactor F_{420} biosynthesis

and characterized the remarkable diversity of mutations in this and 5 other genes involved in

1

nitroimidazole activation. We show that $F_{420}H_2$–deficient nitroimidazole-resistant mutants are hypersusceptible to the selective decontaminant malachite green used in solid media to isolate mycobacteria and may evade detection on such media. These results have important implications for development and clinical use of genotypic and phenotypic methods for nitroimidazole susceptibility testing.

ABSTRACT

Delamanid represents one of two novel antimicrobial classes approved to treat tuberculosis in over 40 years. Pretomanid is another promising nitroimidazole pro-drug in clinical development. Characterization of the full spectrum of mutations conferring resistance to nitroimidazoles and their related phenotypes in *Mycobacterium tuberculosis* will inform development of suitable genotypic and phenotypic drug susceptibility tests. Here, we used a range of pretomanid doses to select pretomanid-resistant mutants in two pathologically distinct murine TB models. The frequency of spontaneous pretomanid resistance mutations was approximately 10^{-5} CFU. Pretomanid demonstrated dose-dependent bactericidal activity and selective amplification of resistant mutants. Whole genome sequencing of 161 resistant isolates from 47 mice revealed 99 unique mutations, 90% of which were found in 1 of 5 genes previously associated with nitroimidazole activation and resistance. The remaining 10% harbored isolated mutations in *Rv2983*. Complementing an *Rv2983* mutant with a wild-type copy of *Rv2983* restored wild-type susceptibility to pretomanid and delamanid, confirming that loss of *Rv2983* function causes nitroimidazole resistance. By quantifying F_{420} and its precursor Fo in *Mycobacterium smegmatis* overexpressing *Rv2983* and an *M. tuberculosis Rv2983* mutant, we provide evidence that Rv2983 is necessary for F_{420} biosynthesis and nitroimidazole activation, perhaps as the guanylyltransferase CofC. $F_{420}H_2$-deficient mutants displayed hypersusceptibility to malachite green (MG), a selective decontaminant present in solid media used to isolate and propagate mycobacteria from clinical samples. The wide diversity of mutations causing high-level

pretomanid resistance and MG hypersusceptibility of most mutants poses significant challenges to clinical detection of nitroimidazole resistance using either genotypic or phenotypic methods.

INTRODUCTION

Despite decades of efforts to end the global tuberculosis (TB) epidemic, *Mycobacterium tuberculosis* is the leading killer among infectious agents plaguing mankind (*1*). The emergence and spread of multidrug-resistant (MDR) and extensively drug-resistant (XDR) *M. tuberculosis* makes the eradication effort much more difficult because treatment requires administration of more toxic and less effective second- and third-line drugs for up to 2 years (*1, 2*). Delamanid and pretomanid are promising new bicyclic 4-nitroimidazole drugs that have shown potential in pre-clinical and clinical studies to shorten and simplify the treatment of TB, including drug-resistant forms (*3-9*). Delamanid received conditional approval by the European Medicines Agency (EMA) to treat MDR-TB in 2014 (*10*) and pretomanid is currently being evaluated in Phase 2/3 clinical trials (ClinicalTrials.gov Identifiers: NCT03338621, NCT02589782, NCT02333799, NCT03086486). Particularly notable is a novel regimen comprised of bedaquiline, pretomanid and linezolid that may represent a highly efficacious oral, short-course regimen for treatment of MDR/XDR-TB (*4*)(ClinicalTrials.gov Identifiers: NCT02333799, NCT03086486).

Two non-exclusive mechanisms of action have been described for these bicyclic 4-nitroimidazole drugs: inhibition of cell wall biosynthesis through inhibition of mycolic acid synthesis and respiratory poisoning through release of nitric oxide during bacterial drug metabolism (*11, 12*). Pretomanid and delamanid are prodrugs that require bioreductive activation of an aromatic nitro group by the 8-hydroxy-5-deazaflavin (coenzyme F_{420})-dependent nitroreductase Ddn in order to exert bactericidal activity (*13*). The reaction involves the transfer of two electrons from the reduced form of F_{420} ($F_{420}H_2$) produced by an F_{420}-dependent glucose-6-phosphate dehydrogenase (Fgd1) (*12, 14*). Therefore, F_{420} biosynthesis and reduction are essential for the activation of delamanid, pretomanid and other nitroimidazole prodrugs. Three genes are identified as essential for F_{420}

3

biosynthesis in *M. tuberculosis* complex (*15, 16*). *fbiC* encodes a 7,8-didemethyl-8-hydroxy-5-deazariboflavin (Fo) synthase that catalyzes the condensation of 5-amino-6-ribitylamino-2,4 (1*H*, 3*H*)-pyrimidinedione and tyrosine to form the F_{420} precursor Fo (*17, 18*). *fbiA* encodes a transferase that is believed to catalyze the transfer of a phospholactyl moiety to Fo to generate F_{420}-0, while *fbiB* encodes a F_{420}-0:γ-L-glutamyl ligase that catalyzes the sequential addition of a variable number of glutamate residues to F_{420}-0 to yield coenzyme F_{420}-5 or -6 in mycobacteria (*12*). In the methanogen *Methanocaldococcus jannaschii*, a guanylyltransferase termed CofC is believed to generate an intermediate (L-lactyl-2-diphospho-5'-guanosine,–LPPG) in the F_{420} biosynthesis pathway (*19*). A homologous enzyme, MSMEG_2392, is shown to be necessary for F_{420} synthesis in *Mycobacterium smegmatis* through transposon mutagenesis studies (*20*). An ortholog, *Rv2983*, is present in *M. tuberculosis*. However, the role of MSMEG-2392 and Rv2983 in F_{420} biosynthesis has remained unexplored.

Loss-of-function mutations in *ddn*, *fgd1* and *fbiA-C* causing delamanid and pretomanid resistance are readily selected *in vitro* in *M. tuberculosis* complex (*16, 18, 21-23*). However, the genetic spectrum of mutations emerging during *in vivo* selection has not been characterized. In order to study bacterial genetic, host and pharmacological factors associated with emergence of nitroimidazole resistance *in vivo*, we selected pretomanid-resistant mutants using a wide range of pretomanid doses in two mouse models of TB and characterized them by whole genome sequencing (WGS). Because the lungs of TB patients feature a heterogeneous array of lesion types associated with diversified immune responses and drug penetration (*24, 25*), we used both C3HeB/FeJ mice, which develop caseating lung lesions in response to *M. tuberculosis* infection, and BALB/c mice, which do not, to investigate the impact of these caseating lesions and their associated micro-environments on mutant selection. In the present study, we found that pretomanid-resistant mutants were readily selected by monotherapy in both mouse strains. While the majority of resistant isolates harbored isolated mutations in genes previously associated with

nitroimidazole resistance, all the resistant isolates lacking such mutations had mutations in *Rv2983*. We went on to confirm that loss-of-function mutations in *Rv2983* cause high-level pretomanid and delamanid resistance through disruption of F_{420} biosynthesis, supporting the hypothesis that *Rv2983* plays a role similar to *cofC* in *M. tuberculosis*. Furthermore, $F_{420}H_2$-deficient nitroimidazole-resistant *M. tuberculosis* mutants, including *Rv2983* mutants, were found to be hypersensitive to malachite green (MG), an organic compound used as a selective decontaminant in solid media for culturing *M. tuberculosis*, which may have important implications for their detection in clinical samples.

MATERIALS AND METHODS

Bacterial strains, media, antimicrobials and reagents. Wild type *M. tuberculosis* H37Rv (ATCC 27294) was mouse-passaged, frozen in aliquots and used in all the experiments. The wild type *M. smegmatis* strain mc^2 155 was obtained from the stock in the lab. Unless stated otherwise, Middlebrook 7H9 medium (Difco, BD) supplemented with 10% oleic acid-albumin-dextrose-catalase (OADC) complex (BD), 0.5% glycerol and 0.05% Tween 80 (Sigma-Aldrich) (7H9 broth) was used for cultivation. Middlebrook 7H10 agar and selective 7H11 agar (Difco, BD), prepared from powder and containing 10% OADC and 0.5% glycerol, were used for comparison of strain recovery on commercially available agar plates. Lowenstein Jensen (LJ) slants were purchased from BD. Pretomanid and delamanid were kindly provided by the Global Alliance for TB Drug Development (New York, NY).

Mouse infection models and pretomanid treatment. All animal procedures were approved by the Animal Care and Use Committee of Johns Hopkins University. Aerosol infections were performed using the Inhalation Exposure System (Glas-col Inc., Terre Haute, IN), as previously described (*26*). Briefly, 6-week-old female BALB/c mice (Charles River, Wilmington, MA) and

5

C3HeB/FeJ mice (Jackson Laboratories Bar Harbor, ME) were infected with a log phase culture of *M. tuberculosis* that was grown in 7H9 broth to O.D.600_{nm} = 1.0 and then diluted in the same medium prior to infection to deliver 50-100 CFU to the lungs. Pretomanid was formulated for oral administration as previously described (*27*). Beginning 8 weeks after aerosol infection, mice were randomly allocated into groups and treated once daily (5 days per week) for up to 8 weeks with pretomanid at doses of 10, 30, 100, 300 and 1000 mg/kg. Untreated mice were sacrificed on the day after aerosol infection and on the day of treatment initiation to determine the number of CFU implanted in the lungs and pretreatment CFU counts, respectively. Additional mice were sacrificed after 3 and 8 weeks of treatment to evaluate the treatment response. Serial 10-fold dilutions of lung homogenates were plated on 7H11 agar. Week 8 samples including those from untreated mice were also plated in parallel on 7H11 plates containing 0.25, 1 and 10 µg/ml of pretomanid to quantify the resistant CFU. Plates were incubated at 37°C for 28 days before final CFU counts were determined.

Whole genome sequencing. For each mouse lung that yielded growth on pretomanid-containing plates, individual colonies and, for a subset of mice, pools of up to 15 colonies, were randomly selected from pretomanid-containing plates and sub-cultured in 7H9 broth prior to extraction of genomic DNA using the cetyltrimethylammonium bromide (CTAB) protocol (*28*) and vortexing (Genegate, Inc.). 2-3 µg of genomic DNA was sheared by a nebulizer to generate DNA fragments. The DNA library was prepared using a genomic DNA sample preparation kit (Illumina, Inc.), in which adapter-ligated DNA fragments were 250-350 bp in length, and carried out on an Illumina Genome Analyzer II (Illumina, Inc). The sequencer was operated in paired-end mode to collect pairs of reads of 51-bp from opposite ends of each fragment. Image analysis and base-calling were done by using the Illumina GA Pipeline software (v0.3). The reads that were generated for each strain were aligned to the reference genome of *M. tuberculosis* H37Rv (*29*). Based on alignment to the corresponding region in the reference genome, single nucleotide polymorphism

6

(SNP), insertion and deletion were identified on the genome of resistant strains by using a contig-building algorithm to construct a local ~200 bp sequence spanning the site of mutagenesis (*30*). Distribution of mutation type and mutation frequency in genes involved in nitroimidazole resistance was calculated by counting the total number of unique mutations isolated from each mouse in the same treatment group.

Complementation of an *Rv2983* mutation. A 1,044-bp DNA fragment containing the open reading frame (ORF) of the wild type *Rv2983* gene, including 340 bp of 5'-flanking sequence and 59 bp of 3'-flanking sequence, was PCR-amplified from *M. tuberculosis* H37Rv genomic DNA using primers *Rv2983*-1F and *Rv2983*-1R (Table S1). The *Rv2983* PCR product was ligated into XbaI-digested *E. coli*-mycobacterium shuttle vector pMH94 (*31*) using NE builder HiFi DNA assembly kit (NE Biolabs) to generate the recombinant pMH94-*Rv2983* vector. Similarly, a 388-bp DNA fragment containing the *hsp60* promoter and a 645-bp DNA fragment of *Rv2983* open reading frame were amplified from *M. tuberculosis* H37Rv genomic DNA using primer sets *hsp60*-F and *hsp60*-R and *Rv2983*-2F and *Rv2983*-2R, respectively (Table S1), and ligated into XbaI-digested *E. coli*-mycobacterium shuttle vector pMH94 to yield pMH94-*hsp60*-*Rv2983*. A small amount of ligation reaction was transferred into *E. coli* competent cells, followed by DNA sequencing of the inserts in the corresponding recombinants. The recombinants pMH94-*Rv2983* and pMH94-*hsp60*-*Rv2983* were electroporated into competent cells of *Rv2983* mutant strain BA_101 (B101), harboring an A198P substitution, to enable selection of complemented candidates B101p*Rv2983* and B101p*hsp60*-*Rv2983* on 7H10 agar containing 25 µg/ml of kanamycin. To confirm the complementation genetically, Southern blotting was performed using a digoxigenin (DIG) DNA labeling and detection kit according to the manufacturer's protocol (Sigma). Briefly, a 448-bp *Rv2983* probe was generated by addition of DIG-dUTP (Sigma) to PCR reactions containing primer pairs *Rv2983*-3F and *Rv2983*-3R (Table S1). Acc65I-digested (NE biolabs) genomic DNA of the wild type, the B101 mutant and the B101p*Rv2983* and B101p*hsp60*-

Rv2983 complemented strains was separated on agarose gel and transferred onto positively-charged nylon-membrane (GE). After pre-hybridization, the membrane was hybridized with the DIG-labeled *Rv2983* probe at 68°C overnight, followed by addition of anti-DIG alkaline phosphatase conjugate. After stringent washes, the membrane was incubated with the chemiluminescence substrate disodium 3-(4-methoxyspiro {1,2-dioxetane-3,2(5′-chloro)tricycloecan}-4-yl)phenyl phosphate (CSPD) and exposed on X-ray film in a dark room prior to development using a developer (AFP imaging)(*32*).

MIC determination. Log-phase cultures were diluted to achieve a bacterial density of approximately 10^5 CFU/ml in conical tubes containing 7H9 broth without Tween 80. Serial 10-fold dilutions were plated on 7H11 agar containing stepwise 2-fold increasing pretomanid concentrations ranging from 0.015 to 64 µg/ml or delamanid concentrations from 0.001 to 1.024 µg/ml. Drugs were initially dissolved in dimethylsulfoxide (DMSO) (Sigma) prior to further dilution in 7H9 broth or 7H11 agar. Cultures were incubated at 37°C for 14 days or 28 days after plating. MIC was defined as the lowest drug concentration that inhibited visible *M. tuberculosis* growth in conical tubes or that inhibited 99% of CFU growth on pretomanid-containing plates (*33, 34*). The experiments were repeated twice.

Construction of recombinants overexpressing *Rv2983*, with or without *fbiC*, in *M. smegmatis*. A 645-bp DNA fragment containing the *Rv2983* ORF was PCR-amplified from *M. tuberculosis* H37Rv genomic DNA using primers *Rv2983*-4F and *Rv2983*-4R (Table S1). The amplified PCR product was ligated into the NdeI- and PacI-digested *E. coli*-mycobacterium shuttle vector pYUBDuet (*35*) using NE builder HiFi DNA assembly kit (NE Biolabs) and then transferred into Turbo-competent *E. coli* cells (NE Biolabs) prior to plating on LB agar plates containing 100 µg/ml of hygromycin B for selection of recombinants. The *Rv2983* PCR product was also similarly ligated into the same NdeI- and PacI-digested pYUBDuet vector harboring

8

fbiC (termed p*fbiC*) (*35*) to overexpress both *Rv2983* and *fbiC*. After confirmation by restriction digestion and DNA sequencing, the constructs were electroporated into competent *M. smegmatis* cells prior to selecting recombinants on 7H10 agar plates containing 100 µg/ml of hygromycin B. PCR amplification was used to confirm the inserts on the *M. smegmatis* genome. pYUBDuet and pYUBDuet harboring *fbiA, fbiB and fbiC* (termed p*fbiABC*) (*35*) were also transferred into competent *M. smegmatis* cells to serve as controls.

Measurement of Fo and F_{420}. Extraction of Fo and F_{420} was performed in *M. smegmatis* and *M. tuberculosis* strains according to a previous study (*35*), with minor modifications. Briefly, *M. smegmatis* strains harboring different constructs and pYUBDuet were grown in 7H9 broth in a shaker to mid-log phase (O.D.$_{600nm}$ = 0.7-1.0), followed by induction using 1mM isopropyl β-D-1-thiogalactopyranoside (IPTG) for 6 and 26 hours. After centrifugation for 15 min at 16000 x g, the supernatants were removed for detection of Fo, which is principally found in culture supernatant whereas F_{420} with 5 or 6 glutamate residues is largely retained inside cells (*15, 35, 36*). The cell pellets were washed with 25mM sodium phosphate buffer (pH 7.0) and re-suspended at 100 mg/mL in the same buffer, then autoclaved at 121°C for 15 min. After centrifugation at 16000 x g for 15 min at 4°C, the cell extracts were harvested for detection of F_{420} (*35*). Fluorescence of the supernatant and cell extracts was measured using an excitation wavelength of 410 nm and an emission wavelength of 465 nm. Fluorescent signals of Fo were normalized using the O.D. at 600nm. The small portion of Fo (1-7%) retained inside cells was ignored when quantifying F_{420} in cell extracts (*37*). Relative fluorescent signals were calculated in *M. smegmatis* harboring each of recombinants relative to pYUBDuet alone. Similarly, cell extracts and supernatant were extracted from *M. tuberculosis* strains grown in 7H9 broth for 6 days at initial O.D.$_{600nm}$ of 0.1. Relative fluorescent signals of F_{420} and Fo were calculated using cell extracts and supernatant relative to 25 mM phosphate buffer and 7H9 broth, respectively. *M. smegmatis* harboring pYUBDuet-*fbiABC*

9

was used as a positive signal control for Fo and F_{420} due to their commercial unavailability (*35*). The experiment was repeated twice.

Quantification of gene expression in *M. tuberculosis*. 6-day-old *M. tuberculosis* strains grown in 7H9 broth as described above were sub-cultured in fresh 7H9 at O.D.$_{600nm}$ = 0.05 followed by incubation at 37°C in a shaker for 2 and 4 days. Bacterial pellets were collected by centrifugation at 3500 rpm at 4°C for purification of total RNA using Trizol (Thermo Fisher Scientific) according to the manufacturer's protocol followed by removal of DNA contamination with Turbo DNAse (Ambion). Following cDNA synthesis with random hexamers and oligo(dT)20 primer and superscript III reverse transcriptase (Invitrogen), quantitative PCR was performed to measure gene expression of *M. tuberculosis* using SYBR Green PCR master mix (Thermo scientific) and StepOne^{TM} system (Applied biosystems) with primer sets listed in Table S1. The cycle threshold value (C_T) measured for each gene was normalized to that of the housekeeping gene *sigA* (ΔC_T) amplified by the primers *sigA*-F and *sigA*-R (Table S1). $\Delta\Delta C_T$ was calculated in each of pretomanid-resistant strains relative to the wild-type H37Rv prior to calculation of the fold-change in gene expression ($2^{\wedge}-\Delta\Delta C_T$) (*38*). All samples were prepared in duplicate. PCR was performed from an equal amount of cDNA samples synthesized with oligo(dT)20 with primers *fbiC*-5-7_F and *fbiC*-5-7_R (Table S1) using the Q_5 High-fidelity PCR kit (New England Biolabs) and C1000 Thermal cycler (Biorad). The PCR product was examined by electrophoresis on a 1% agarose gel.

Malachite green susceptibility testing. 7H9 media supplemented with 10% OADC, 0.5% glycerol, 1.5% Bacto^{TM} Agar (BD) and malachite green (MG) oxalate (Alfa Aesar) was used to prepare solid 7H9 media with differing MG concentrations. *M. tuberculosis* strains were grown to mid-log phase and diluted to OD$_{600nm}$ = 0.1 in 7H9 broth before serial 10-fold dilutions were plated in 100 or 500 µl aliquots on 7H9 agar containing MG concentrations of 0, 0.1, 0.3, 1, 3, 10, 30,

100, 300, 1000 µg/ml or 0, 3, 6, 12 µg/ml. CFU were counted after 28, 35 and 49 days of incubation. The same cultures were also plated on 7H10 and 7H11 agar plates and LJ slants. Serially diluted cultures were inoculated onto LJ slants using calibrated disposable inoculating loops (10 µl per loop, BD) as one loop per LJ slant. Plates were incubated at 37°C for 21, 28 and 35 days for CFU counts. Colony size was observed weekly until day 35, beginning 21 days after plating. The experiment was repeated two times under similar conditions.

Statistical analysis. Log_{10}-transformed CFU counts, fold-change values of gene expression and absorbance (A_{410}) values of fluorescent signals were used to calculate means and standard deviations for each data set. Differences between means were compared by the Student's *t* test in Microsoft Excel. Differences in mutation frequencies between two mouse models were evaluated by Fisher's exact test in GraphPad Prism 6. A *p*-value of < 0.05 was considered statistically significant.

RESULTS

Spontaneous pretomanid-resistant mutants exist at a relatively high frequency in infected mice and are selectively amplified by treatment with active doses of pretomanid.
To study the dose-response of pretomanid and explore the genetic spectrum of nitroimidazole resistance selected *in vivo*, we established chronic *M. tuberculosis* infections in BALB/c and C3HeB/FeJ mice and then treated with a range of pretomanid doses for up to 8 weeks. Despite lower CFU counts on the day after infection (W-8) in C3HeB/FeJ mice (1.67 $\log_{10}$ CFU per lung) compared to BALB/c (2.26 $\log_{10}$) (*p* <0.001), higher CFU counts were observed in C3HeB/FeJ mice 8 weeks later on the day treatment started (D0) and after 3 weeks of treatment in almost all groups (*p* <0.001 - 0.05) (Fig. 1A). Three C3HeB/FeJ mice treated with 1000 mg/kg required euthanasia during the second week of treatment, prompting a dose reduction from 1000 mg/kg to 600 mg/kg in both strains. Nevertheless, a clear pretomanid dose-response relationship was

11

observed in both mouse strains after 3 weeks of treatment (Fig. 1A). The three remaining C3HeB/FeJ mice treated with 600 mg/kg beyond the week 3 time point were euthanized after 5 weeks of treatment due to toxicity. One had no detectable CFU and two had ≤ 2.0 $\log_{10}$ CFU of pretomanid-resistant *M. tuberculosis*. After 8 weeks of treatment, total CFU counts fell in a dose-dependent manner in BALB/c mice before a plateau was reached at doses ≥ 300 mg/kg, where resistant CFU were higher and replaced the susceptible CFU ($p < 0.05$) (Fig. 1B). Spontaneous pretomanid-resistant CFU comprised approximately 10^{-5} of the total CFU in the absence of drug pressure in untreated BALB/c mice and the proportion of the total CFU that was comprised of pretomanid-resistant CFU increased with dose up to the 300 mg/kg dose group. Dose-dependent bactericidal activity was also observed in C3HeB/FeJ mice (Fig. 1C). However, selective amplification of pretomanid-resistant mutants was more extensive and occurred at lower doses than in BALB/c mice (Fig. 1B and 1C). We were not able to measure the spontaneous frequency of resistant mutants in untreated C3HeB/FeJ mice because they succumbed to infection prior to week 8. Pretomanid-resistant CFU replaced susceptible CFU in C3HeB/FeJ mice receiving doses as low as 30 mg/kg and pretomanid-resistant CFU counts were roughly 10 times higher in C3HeB/FeJ mice compared to BALB/c mice (Fig. 1B and C), which indicates greater potential for selective amplification of pretomanid resistance with monotherapy in this strain. Most resistant isolates grew on plates containing 10 µg/ml of pretomanid, but some had fewer CFU on plates containing 10 µg/ml than on those containing 1 µg/ml of pretomanid.

Whole genome sequencing of pretomanid-resistant mutants revealed diverse mutations in *Rv2983* or in one of five other genes required for pretomanid activation.

To characterize mutations associated with pretomanid resistance *in vivo*, we performed WGS on 136 individual pretomanid-resistant colonies and 25 colony pools picked from 47 individual mice harboring pretomanid-resistant CFU after 8 weeks of treatment (Table S2 and S3). Each individual isolate had an isolated mutation in *Rv2983* or one of the 5 genes previously shown to

12

be required for pretomanid activation. Overall, 99 unique mutations in these 6 genes were identified from individual and pooled isolates (Table 1 and 2). Except for mutations K9N (*fgd1*), R322L (*fbiC*) and Q120P (*fbiA*), which were shared by two mice each, no two mice harbored the same mutation, which emphasizes the large target size for resistance-conferring mutations. In both BALB/c and C3HeB/FeJ mice, more than half of the resistant isolates were *fbiC* mutants (54 and 56%, respectively) (Table 3). For the other five genes, the rank order by mutation frequency was *Rv2983* (15%) > *fbiA* (13%) > *ddn* (9%) > *fbiB* (6%) > *fgd1* (4%) in BALB/c mice and *fbiA* (18%) > *ddn* (16%) > *fgd1* or *Rv2983* (4%) > *fbiB* (2%) in C3HeB/FeJ mice. No significant differences in mutation frequencies between BALB/c and C3HeB/FeJ mice were observed, although a trend towards more *Rv2983* mutations in BALB/c mice (8/54, 15% of all mutations) compared to C3HeB/FeJ mice (2/45, 4%) was detected. The mutations identified in *Rv2983* included 8 point mutations resulting in the following amino acid substitutions: R25S, R25G, A68E, A132V, G147C, C152R, Q114R and A198P, as well as an insertion of C after A27 and a deletion of I129 (-ATC) (Tables 1 and 2). The overall frequency distribution of unique mutations was as follows: *fbiC* (55%, *n* = 54), *fbiA* (15%, n = 15), *ddn* (12%, n = 12), *Rv2983* (10%, n=10), *fgd1* (4%, *n* = 4), and *fbiB* (4%, n=4) (Fig. 2 and Table S4). There were no clear associations between pretomanid dose and the mutated gene. Mutations in *fbiC* comprised a higher proportion of those selected in our *in vivo* study compared to the proportion selected in a previous in *vitro* study (26%, *p* = 0.0001)(*22*). On the other hand, mutations in *ddn* (29%) were more frequent after *in vitro* selection than in our mouse models (12%) (*p* =0.001). *In vitro* mutation frequencies for *fbiA*, *fgd1* and *fbiB* (19%, 7% and 2%, respectively) were similar to our findings in mice.

Among the 99 unique mutations, all but one (an IS6110 insertion located in 85-bp upstream of the *fbiC* coding sequence in isolate KA-026a (Table 2 and Table S2) were found within the coding regions of the six genes. In total, 54% (53/99) were non-synonymous point mutations (no synonymous point mutations were identified), 35% (35/99) were insertions or deletions (indels),

13

and 11% (11/99) were substitutions resulting in a stop codon. No significant difference in the distribution of point mutation and indels was found between ours and the *in vitro* study by Haver, *et al*, in which non-synonymous point mutations and indels were 50% (75/151) and 24% (36/151), respectively. However, the frequency of stop codon substitutions in the latter study (26%, 40/151) was higher than that observed in the present study (11%, 11/99) (p = 0.004), 85% (34/40) of which were in *ddn* in the latter study (*22*). Non-synonymous point mutations predominated relative to indels and stop codon mutations overall and in each gene except for *ddn* (Fig. 2 and Table S4). The frequency of point mutations was similar between BALB/c and C3HeB/FeJ mice (56% versus 51%) (Table 3). A higher frequency of indels occurred in C3HeB/FeJ compared to BALB/c mice (44% versus 28%), while more stop codon mutations occurred in BALB/c, but these differences were not statistically significant. There was no clear association between dose of pretomanid and the type of mutation selected.

Comparing the 99 unique mutations identified in our study with the 151 unique mutations in 5 of the same genes selected *in vitro* (*22*), only 4 mutations were found in the same position. Only W79 stop (*fbiA*) and N336K (*fbiC*) mutations were found in both datasets while both T273 and H190 (*fbiC*) were mutated in the same position but with different mutations. As expected from the fact that most mutants could be isolated on plates containing 10 μg/ml of pretomanid, MICs determined against a small subset of isolates indicated high-level pretomanid resistance (Table S5 and Table 1 and 2). Taken together, these data illustrate the tremendous diversity of mutations capable of conferring high-level pretomanid resistance.

Mutations in *Rv2983* cause resistance to pretomanid and delamanid.

To prove that mutations in *Rv2983* are sufficient for nitroimidazole resistance, merodiploid complemented strains were constructed by introducing a copy of the wild type *Rv2983* gene into B101, an *Rv2983* mutant (A198P), through site-specific integration (*31, 32*). Following

confirmation of successful integration by Southern blot using a DIG-labeled *Rv2983* probe (Figs. S1A and S1B), susceptibility testing by 7H9 broth dilution confirmed significantly higher nitroimidazole MICs against the *Rv2983* mutant (pretomanid and delamanid MICs of 32 μg/ml and 0.064-0.128 μg/ml, respectively) and full restoration of susceptibility in the complemented strains (pretomanid and delamanid MICs of 0.25 μg/ml and 0.008 μg/ml, respectively).

$Rv2983$ is required for F_{420} biosynthesis.

To demonstrate that *Rv2983* is required for F_{420} biosynthesis, we measured the production of Fo and F_{420} in *M. smegmatis* strains overexpressing *Rv2983* and in *M. tuberculosis Rv2983* mutant strains compared with their corresponding control strains. *Rv2983* and *fbiC* were successfully cloned into pYUBDuet and p*fbiC* (designated p*Rv2983* and p*fbiC-Rv2983*, respectively), followed by successful transformation of *M. smegmatis*, along with pYUBDuet and p*fbiABC*, which were confirmed by restriction enzyme digestion, DNA sequencing and PCR amplification (data not shown). Overexpression of *Rv2983 in M. smegmatis* increased F_{420} production but resulted in little change in Fo production compared to the control strain after 6 and 26 hours of induction with IPTG (Figs. 3A and 3B). As expected, mutation of *Rv2983* in the *M. tuberculosis* B101 mutant markedly reduced F_{420} production, resulting in accumulation of Fo. Complementation fully restored the wild-type phenotype (Figs. 3C and 3D). In order to evaluate the method, we also overexpressed *fbiC*, which encodes the Fo synthase, with and without concomitant overexpression of Rv2983 in *M. smegmatis*. As expected, overexpression of *fbiC* increased Fo and, consequently, F_{420} concentrations. Relative to the control strain, F_{420} concentrations were similar when either *fbiC* or *Rv2983* was over-expressed alone (Fig. 3A). Interestingly, when *Rv2983* was co-overexpressed with *fbiC*, a dramatic increase in F_{420} was observed relative to over-expression of either gene alone (3.4 and 3.1-fold, respectively) after 6 hours of IPTG induction ($p<0.001$), with corresponding significant decreases of Fo levels after 6 and 26 hours of IPTG induction (5.8 and 3.1-fold; $p<0.005$ and 0.05, respectively) (Fig. 3A and 3B). These results

15

suggest that the excess Fo produced by *fbiC* over-expression was efficiently converted to F_{420} by over-expressed Rv2983. On the other hand, although a small amount of F_{420} was observed in cell extracts of two *Rv2983* point mutants (B101 [A198P] and KA016 [Q114R]), their F_{420} content was significantly lower than that of the wild type (7.3 and 7.7-fold) ($p < 0.001$) and complemented B101 mutant (Fig. 3C). As expected, Fo accumulated in the two *Rv2983* mutant strains relative the wild-type (6.7 and 6.5-fold; $p<0.05$ and 0.005, respectively) (Fig. 3D), indicating that Fo was not efficiently converted to F_{420} in the presence of a mutated *Rv2983*. Two other pretomanid-resistant strains were also assessed as controls. The KA026 mutant with an IS6110 insertion 85 bp upstream of *fbiC* had undetectable Fo and very little F_{420} content, while the KA91 mutant with an IS6110 insertion at amino acid position 108 of Ddn showed a wild-type phenotype with respect to F_{420} and Fo concentrations (Fig.3C and D).

To understand the effect of mutations on gene expression and its regulation, we performed RT-qPCR after sub-culturing the *M. tuberculosis* strains in fresh 7H9 broth. Expression of *Rv2983* and *fbiC* increased 2.4- and 1.6-fold, respectively, in the *Rv2983* mutant B101 relative to the wild-type H37Rv parent after 4 days of incubation in 7H9 broth. Similar increases were observed in other genes such as *fbiA* (2.3-fold), *fbiB* (2.0-fold) and *fgd1* (2.2-fold) involved in F_{420} biosynthesis, suggesting that the reduced F_{420} content caused by the *Rv2983* A198P mutation resulted in upregulation of the F_{420} biosynthesis pathway (Fig. S2A). Expression of *fbiC* in the KA026 mutant decreased 114-fold compared to that in the wild-type H37Rv parent after 2 days of incubation in 7H9 broth, likely resulting from interrupted *fbiC* transcription as a result of the insertion IS6110 at 85-bp upstream and explaining the low levels of both Fo and F_{420} in that mutant (Fig. S2 B). A faint band representing the *fbiC* DNA fragment of 937-bp from the *fbiC* KA026 mutant relative to H37Rv further supports this conclusion (Fig. S2C).

F_{420}-deficient pretomanid-resistant mutants are attenuated for growth in the presence of malachite green.

Previous work using *M. smegmatis* showed that mutations in MSMEG_5126 (homolog of *fbiC*) and MSMEG_2392 (which shares 69% homology with *Rv2983*) reduce the ability to decolorize and detoxify MG, indicating that F_{420} is necessary for this process (*20*). To evaluate the role of each gene associated with nitroimidazole activation in the susceptibility to MG, log-phase cultures of 10 selected mutants were plated on 7H9 agar supplemented with a range of MG concentrations. All mutants deficient in F_{420} synthesis or reduction (*i.e.*, those with mutations in *fbiA-C, Rv2983* or *fgd1*) were more susceptible to MG, while the *ddn* mutant retained the same susceptibility as the wild type H37Rv parent, whose growth was almost completely inhibited at MG concentrations ≥ 30 µg/ml (Fig. 4A). The lability of $F_{420}H_2$ and lack of a commercial source for F_{420} made it unfeasible to attempt to test whether provision of $F_{420}H_2$ could rescue the MG-hypersusceptible phenotype of the $F_{420}H_2$-deficient mutants. To confirm that *Rv2983* is necessary for the intrinsic resistance of *M. tuberculosis* to MG, we compared the growth of the B101 mutant to that of the wild type and complemented strains on MG. Again, growth of this *Rv2983* mutant was inhibited by lower concentrations of MG than the wild type strain and required longer incubation times before colonies appeared on MG-containing plates (Fig. 4B-D). Plating at higher bacterial density (500 µl rather than 100 µl of cell suspension per plate) significantly increased recovery (Fig. S3A and B). Complementation of *Rv2983* fully restored the wild-type growth phenotype on MG concentrations up to 6 µg/ml. Interestingly, at MG concentrations above 6 µg/ml, greater recovery was observed when *Rv2983* was expressed behind the native promoter compared to the *hsp60* promoter (Fig. 4B-D). Smaller colony size was observed in the *Rv2983* mutant relative to the wild type and the complemented strains on plates without MG after 21 days of incubation but not after 28 days of incubation (Fig. 5). However, smaller colony size and deficient decolorization was observed for the *Rv2983* mutant on plates containing MG concentrations as low as 0.25 and 1 µg/ml, even after 28 days of incubation (Fig. 5). At MG concentrations of 6-12 µg/ml, even more-concentrated aliquots of the B101 mutant culture showed markedly reduced recovery despite 42 days of incubation (Fig. 5).

17

Because all solid media commonly used to isolate and cultivate *M. tuberculosis* in clinical laboratories contain MG as a selective decontaminant, the increased MG susceptibility conferred by mutations in *fbiA-C*, *Rv2983* and *fgd1* could compromise the isolation and propagation (and hence identification) of nitroimidazole-resistant mutants from clinical samples. Commercial 7H10 agar, 7H11 agar and LJ medium contain 0.25, 1 and 400 µg/ml, respectively, of MG. To assess the potential impact of these media on the isolation of an $F_{420}H_2$-deficient nitroimidazole-resistant *Rv2983* mutant relative to an $F_{420}H_2$-sufficient, but still nitroimidazole-resistant, *ddn* mutant and the nitroimidazole-susceptible wild type and *Rv2983*-complemented mutant, we inoculated these media in parallel using serial dilutions of each strain. The *Rv2983* mutant exhibited 10 times lower CFU counts and smaller colony size relative to other strains after 21 and 28 days of incubation on 7H10 agar plates (p <0.01) (Figs. 6A and C(a)). The result after 35 days of incubation was generally similar between the mutant and the control strains (Fig. 6A and C(b)). A similar semi-quantitative growth assessment of the *Rv2983* mutant on LJ media compared to other strains including a *ddn* mutant (K91, IS6110 ins in D108) revealed growth inhibition of the *Rv2983* mutant that was ameliorated by increasing the size of the bacterial inoculum from 10^2 to 10^6 CFU/ml and increasing the incubation time from 28 to 35 days (Fig. 6D). Interestingly, no difference in growth was found on 7H11 agar (Fig. 6B), even when comparing colony size after just 21 days of incubation (Fig. 6C(c)), despite higher MG concentrations in that medium compared to 7H10. Unlike 7H10, 7H11 medium contains hydrolysate of casein, which may somehow mitigate against the MG toxicity. Taken together, these results indicate that use of 7H10 and LJ could compromise the recovery and propagation of $F_{420}H_2$-deficient nitroimidazole-resistant mutants from clinical specimens and that 7H11 agar may be the preferred solid media for processing specimens propagating any isolates from nitroimidazole-treated patients.

DISCUSSION

As representatives of one of only two new drug classes approved for use against TB in roughly 50 years, delamanid and pretomanid are important and promising new drugs (*3, 4, 6, 7, 39*). The former received accelerated approval from the EMA for treatment of MDR-TB and is now used clinically, albeit sparingly, while a phase 3 trial is being completed. The latter is being evaluated in clinical trials as a component of highly promising regimens for both drug-susceptible and MDR/XDR-TB. Comprehensive knowledge of genetic mutations conferring nitroimidazole resistance in *M. tuberculosis* and the resultant mutant phenotypes are critical for timely and accurate diagnosis of resistance and, therefore, the safe and effective use of these drugs in the clinical setting. Previous work identified 5 genes (*fbiA-C*, *fgd1*, and *ddn*) involved in the activation pathway of nitroimidazole prodrugs in which mutations may confer drug resistance in *M. tuberculosis* complex (*16, 18, 21-23, 40*). In a prior study of the spectrum of nitroimidazole resistance-conferring mutations, Haver, *et al* found that 151 (83%) of 183 pretomanid-resistant isolates selected *in vitro* harbored a single mutation in one of these 5 genes (*22*). However, 17% of the selected strains harbored no mutations in these genes. The present study has several important new findings. First, we identified a novel nitroimidazole resistance determinant—mutations in *Rv2983*—that explained, in the case of our study, all of the pretomanid resistance that was not attributable to mutations in the 5 previously described genes. Second, we demonstrate for the first time that *Rv2983* is required for F_{420} biosynthesis and likely plays a role similar to *cofC* in the methanogen *M. jannaschii* (*19*). Third, we show that *Rv2983* and the ability to produce $F_{420}H_2$ are essential for full tolerance of *M. tuberculosis* to the selective decontaminant MG, which raises serious concerns about the ability to reliably recover most nitroimidazole-resistant mutants from clinical samples on the most widely used microbiology media.

Our study provides the first comprehensive analysis of the spectrum of nitroimidazole-resistant mutants selected *in vivo* and, because we used WGS, it represents the most comprehensive

19

analysis made to-date. Despite the insignificant differences in mutation frequencies between the two mouse strains for other genes related to nitroimidazole activation, *Rv2983* mutations were observed with a somewhat higher frequency in BALB/c mice, indicating a possible host-specific fitness cost that warrants further dedicated study. Like the *in vitro* study by Haver *et al* (*22*), we found that isolated mutations in *fbiA-C*, *fgd1*, or *ddn* explained the majority of the pretomanid-resistant isolates we selected. However, whereas their study left 17% of resistant isolates unexplained, we found that all of the remaining resistant isolates, representing 10% of the total number of unique mutations, harbored mutations in *Rv2983*, a gene not previously implicated in nitroimidazole resistance. Indeed, the proportion of resistant isolates explained by *Rv2983* (10%) was similar to the proportion explained by *fbiA* (15%) and *ddn* (12%) mutations, which lagged only mutations in *fbiC* (55%) as the predominant cause of pretomanid resistance in our mice. Although the *Rv2983* A198T mutation caused a smaller upward shift in the delamanid MIC compared to the pretomanid MIC, the delamanid MIC of 0.064-0.128 µg/ml against the mutant was still significantly higher than the recently proposed critical concentration of 0.016 µg/ml (*41*). Thus, the identification of *Rv2983* mutations should be included in rapid molecular drug susceptibility tests and algorithms for the diagnosis of nitroimidazole resistance from genome sequence data. The 10 mutations in *Rv2983* identified in this study (Table 1 and 2) represent the first step in the process of identifying specific resistance-conferring mutations to inform test development.

Rv2983 has 22% amino acid sequence identity to CofC (MJ0887) of *M. jannaschii*, a putative guanylyltransferase involved in the biosynthesis of coenzyme F_{420} from the precursor Fo. CofC is believed to catalyze the condensation of 2-phospho-L-lactate (LP) and GTP to form lactyl-2-diphospho-5'-guanosine (LPPG) and PP_i (*19*). Subsequent condensation of LPPG with Fo catalyzed by CofD (FbiA) forms F_{420}–0 and is followed by sequential addition of glutamate residues by CofE (FbiB) to produce F_{420} with a poly-glutamate tail (*19*). Up to now, a CofC homolog

20

has not been identified in *M. tuberculosis*. It is known that Fo biosynthesis is catalyzed by FbiC, but it is not clear how Fo is modified by FbiA to form F_{420}–0. Bashiri, *et al* tried to understand the mechanism by overexpressing *fbiC* in the saprophyte *M. smegmatis*, which did not dramatically increase F_{420} biosynthesis, suggesting that an additional intermediate is required to form F_{420}–0 from Fo (*35*). Using overexpression of *Rv2983* in *M. smegmatis* and *M. tuberculosis Rv2983* mutants, we provide initial evidence that Rv2983 catalyzes an important step required for synthesis of F_{420} from Fo in the pathogen *M. tuberculosis*, which adds to previous evidence that its ortholog MSMEG_2392 is involved in F_{420} biosynthesis in *M. smegmatis* (*20*). The validity of the method used in this study for detection of F_{420} and Fo was demonstrated by showing the expected results with two pretomanid-resistant strains, KA016 and KA026, harboring mutations in *fbiC* and *ddn*, respectively. Although the role of *Rv2983* remains to be confirmed, our results confirm that expression of *Rv2983* is necessary for efficient conversion of Fo to F_{420} (Fig. 3G).

Our results confirm and significantly extend prior *in vitro* work demonstrating the remarkable diversity of mutations capable of conferring high-level nitroimidazole resistance. Among the 99 unique mutations we identified in 47 mice, only 3 mutations (K9N in *fgd1*, R322L in *fbiC* and Q120P in *fbiA*) were found in more than one mouse. Furthermore, by comparing the 99 unique mutations observed in our mice with the 151 unique mutations selected *in vitro* (*22*), the same mutation occurred only twice. Thus, each of the 6 genes now implicated in nitroimidazole resistance appears to be devoid of "hot spots" for such mutations. The frequency of spontaneous mutations conferring nitroimidazole resistance in *M. tuberculosis* has been investigated *in vitro* by several studies and found to range from 1 in 10^5 to 7 in 10^7 CFU (*21-23, 27, 40, 42*), which is consistent with our findings in the lungs of untreated BALB/c mice. The large "target size" for mutations in 6 non-essential genes drives these high frequencies of spontaneous nitroimidazole-resistant mutants in *M. tuberculosis* populations, which is as high or higher than that for isoniazid and other TB drugs in clinical use. Our unpublished observations suggest that similar frequencies

of nitroimidazole-resistant mutants exist in sputum isolates collected from treatment-naïve, drug-susceptible TB patients. Delamanid-resistant *M. tuberculosis* has been recovered from patients both before and after delamanid treatment (*10, 43-45*). To date, emergence of resistance has not been described during use of pretomanid in clinical trials, but such use has been restricted to relatively short treatment durations and/or use of highly active companion drugs. Pretomanid resistance has emerged during combination therapy in mouse models (*3, 46*). Thus, the relatively high frequency of spontaneous mutations conferring nitroimidazole resistance and available pre-clinical and clinical data underscore the importance of making validated drug susceptibility testing for this class widely available as clinical usage expands. The unprecedented number and diversity of resistance-conferring mutations demonstrated for nitroimidazole drugs here and by Haver *et al* (*22*), clearly challenges the development and interpretation of rapid molecular susceptibility tests, especially considering that polymorphisms in nitroimidazole resistance genes that represent phylogenetic markers but do not confer pretomanid resistance are well-described (*47, 48*). A similar situation exists for *pncA* mutations and pyrazinamide (PZA) resistance, where an efficient, yet comprehensive method based on saturating mutagenesis for distinguishing single nucleotide polymorphisms conferring resistance was recently described (*49*). A similar analysis of substitutions in the 6 genes related to nitroimidazole resistance would similarly advance the development of drug susceptibility testing using genome sequencing technology.

Amino acid substitutions in the PZA-activating PncA protein that confer PZA resistance are associated with diminished enzymatic activity or reduced abundance of the protein (*49*). Similar mechanisms could explain the overall mechanisms of the 99 mutations we identified in the six genes conferring nitroimidazole resistance. The *Rv2983* A198P or Q114R substitutions may change the conformation of Rv2983 protein structure and reduce its enzymatic activity given that it has no effect on *Rv2983* gene transcription. F_{420} biosynthesis is dramatically decreased while expression of *Rv2983* and other genes increases, perhaps indicating an unknown regulatory

22

mechanism triggered by reduced F_{420} biosynthesis. Mutations identified in *Rv2983* in this study will provide useful information for future studies on structure-function associations of the potential *M. tuberculosis* CofC homolog. The KA026 mutant harboring an IS6110 insertion 85 bp upstream of *fbiC* exhibited significantly decreased expression of *fbiC*, possibly due to interruption of the promoter region, and, consequently, almost complete loss of Fo synthase activity. Hence, the upstream regulatory regions of the six genes also should be considered in future identification of resistance-conferring mutations, although their prevalence in this study was only 1%.

Our findings regarding the heightened susceptibility of $F_{420}H_2$-deficient mutants to MG pose a previously unappreciated challenge to the development and use of phenotypic testing methods. Indeed, we observed reduced or delayed recovery of a nitroimidazole-resistant *Rv2983* mutant on commercial 7H10 and LJ media that include MG as a selective decontaminant (*50*). Since *fbiA-C* and *fgd1* mutants, as well as a second *Rv2983* mutant, exhibited similar hypersusceptibility to MG in 7H9 agar supplemented with MG, their recovery on 7H10 and LJ is also likely to be affected. Selective growth inhibition of nitroimidazole-resistant strains on media that are commonly used in clinical microbiology laboratories around the world raises serious concern that their recovery from clinical specimens may be impaired to such an extent that it reduces the sensitivity and accuracy of phenotypic drug susceptibility testing, especially for isolates comprised of mixed wild-type and resistant populations. This concern is further amplified by the common practice of performing susceptibility testing (including molecular testing), not on primary samples but, on isolates that have been sub-cultured one or more times on solid media. Such practices may drastically reduce the proportion of (or eradicate) $F_{420}H_2$-deficient mutants present in the original sample. In addition, efforts to develop MG decolorization assays for detection of drug-resistant TB are expected to be fruitless for these mutants (*51-54*). We did not determine the basis for the greater recovery of $F_{420}H_2$-deficient mutants on 7H11 vs. 7H10 media despite 4x higher total MG concentrations in the former. The principal differences between these media are the presence of pancreatic digest

23

of casein in 7H11 and lower concentrations of magnesium sulfate countered by the addition of copper sulfate, zinc sulfate and calcium chloride in 7H10. Although this issue clearly requires further study, we presently believe that 7H10 and LJ should not be employed for phenotypic nitroimidazole susceptibility testing and that primary isolation or subculture of any isolate on such media prior to either phenotypic or genotypic susceptibility testing should be avoided whenever possible. When it cannot be avoided, larger inoculum sizes and longer incubation times may increase recovery on 7H10 and LJ. Based on our study, 7H11 agar appears to be the preferred solid medium for recovery of $F_{420}H_2$-deficient nitroimidazole-resistant *M. tuberculosis.*

A role for cofactor $F_{420}H_2$ in tolerance of was previously demonstrated (*20*). Whereas mycobacteria are normally capable of decolorizing and detoxifying MG, mutations in the saprophyte *M. smegmatis* orthologs of *fgd1*, *fbiC* and *Rv2983* disrupt this ability and/or reduce the MIC of MG (*20, 55*). We now extend these observations to the pathogen *M. tuberculosis* and also implicate *fbiA* and *fbiB*, but not *ddn*, in MG tolerance. In *Citrobacter* species, an NADH-dependent triphenylmethane reductase catalyzes reduction of MG to colorless leucoMG that lacks antimicrobial activity and is sequestered in the lipid fraction of the cells (*56, 57*). Triphenylmethane reductase has not been identified in mycobacteria. However, the enhanced MG susceptibility of the $F_{420}H_2$-deficient mutants, but not *ddn* mutants, suggests that one or more analogous, yet unidentified, $F_{420}H_2$-dependent reductases is responsible for decolorizing and detoxifying MG in mycobacteria.

Prior studies indicated other fitness costs associated with $F_{420}H_2$ deficiency, such as hypersusceptibility to oxidative and nitrosative stresses (*12, 58, 59*). Nevertheless, we observed selective amplification of $F_{420}H_2$-deficient mutants in mice over a range of pretomanid doses that included doses producing much higher drug exposures than those produced in patients. Amplification was especially pronounced at higher drug doses, which eliminated the majority of nitroimidazole-susceptible population more effectively, and in C3HeB/FeJ mice. The lack of

24

marked *in vivo* fitness defects is also supported by the fact that the proportion of all unique resistance mutations explained by each mutation did not differ much between the *in vitro* and *in vivo* conditions, except that a higher proportion of *fbiC* mutations predominated in mice, somewhat at the expense of *ddn* mutations (*22*). Likewise, indels and stop codon mutations comprised nearly 50% of the mutations responsible for resistance. This proportion may be biased due to the high drug doses tested in some mice because such mutations are more likely to result in complete loss-of-function and therefore more complete resistance. However, the frequency of such mutations did not appear to change in a dose-dependent manner. Interestingly, most *Rv2983* mutants were selected in BALB/c rather than C3HeB/FeJ mice despite similar mutation rates in other genes between the two mouse strains. Whether this represents a real or a random difference will require further study. Clearly, clinicians must rely on effective combination drug therapy to prevent the selective amplification of nitroimidazole-resistant mutants. Heightened susceptibility to agents causing oxidative stress has been demonstrated for $F_{420}H_2$-deficient *M. tuberculosis* and *M. smegmatis* mutants (*58*). A more complete understanding of the unique vulnerabilities of such mutants should aid in the design of effective combination regimens that also optimally restrict selection of nitroimidazole-resistant mutants.

In conclusion, using BALB/c and C3HeB/FeJ mice and WGS, we characterized the pretomanid dose-response relationships for bactericidal effect and suppression of drug-resistant mutants and profiled the genetic spectrum of pretomanid resistance emerging *in vivo*. A novel resistance determinant, Rv2983, was identified as essential for F_{420} biosynthesis and activation of the novel TB pro-drugs delamanid and pretomanid. Furthermore, we provide evidence that $F_{420}H_2$-deficient, nitroimidazole-resistant *M. tuberculosis* mutants are hypersensitive to MG, raising concern that using MG-containing medium could compromise the isolation and propagation of *M. tuberculosis* from clinical samples and therefore hinder the clinical diagnosis of nitroimidazole resistance. These findings have important implications for both genotypic and phenotypic susceptibility

25

testing to detect nitroimidazole resistance, which will be of increasing importance as wider use of delamanid and, if approved, pretomanid, ensues.

LIST OF SUPPLEMENTARY MATERIALS

Table S1

Table S2

Table S3

Table S4

Table S5

Figure S1

Figure S2

Figure S3

REFERENCES

1. WHO, Global Tuberculosis report. *World Health Organization* **Geneva**, (2017).
2. WHO, Guidelines for the programmatic management of drug-resistant tuberculosis. . *World Health Organization* **Geneva**, (2011).
3. S. Y. Li, R. Tasneen, S. Tyagi, H. Soni, P. J. Converse, K. Mdluli, E. L. Nuermberger, Bactericidal and Sterilizing Activity of a Novel Regimen with Bedaquiline, Pretomanid, Moxifloxacin, and Pyrazinamide in a Murine Model of Tuberculosis. *Antimicrobial agents and chemotherapy* **61**, (2017).
4. R. Tasneen, F. Betoudji, S. Tyagi, S. Y. Li, K. Williams, P. J. Converse, V. Dartois, T. Yang, C. M. Mendel, K. E. Mdluli, E. L. Nuermberger, Contribution of Oxazolidinones to the Efficacy of Novel Regimens Containing Bedaquiline and Pretomanid in a Mouse Model of Tuberculosis. *Antimicrobial agents and chemotherapy* **60**, 270-277 (2015).
5. V. Skripconoka, M. Danilovits, L. Pehme, T. Tomson, G. Skenders, T. Kummik, A. Cirule, V. Leimane, A. Kurve, K. Levina, L. J. Geiter, D. Manissero, C. D. Wells, Delamanid improves outcomes and reduces mortality in multidrug-resistant tuberculosis. *Eur Respir J* **41**, 1393-1400 (2013).
6. M. T. Gler, V. Skripconoka, E. Sanchez-Garavito, H. Xiao, J. L. Cabrera-Rivero, D. E. Vargas-Vasquez, M. Gao, M. Awad, S. K. Park, T. S. Shim, G. Y. Suh, M. Danilovits, H. Ogata, A. Kurve, J. Chang, K. Suzuki, T. Tupasi, W. J. Koh, B. Seaworth, L. J. Geiter, C. D. Wells, Delamanid for multidrug-resistant pulmonary tuberculosis. *N Engl J Med* **366**, 2151-2160 (2012).
7. A. H. Diacon, R. Dawson, F. von Groote-Bidlingmaier, G. Symons, A. Venter, P. R. Donald, C. van Niekerk, D. Everitt, H. Winter, P. Becker, C. M. Mendel, M. K. Spigelman, 14-day bactericidal activity of PA-824, bedaquiline, pyrazinamide, and moxifloxacin combinations: a randomised trial. *Lancet* **380**, 986-993 (2012).
8. R. Dawson, A. H. Diacon, D. Everitt, C. van Niekerk, P. R. Donald, D. A. Burger, R. Schall, M. Spigelman, A. Conradie, K. Eisenach, A. Venter, P. Ive, L. Page-Shipp, E. Variava, K. Reither, N. E. Ntinginya, A. Pym, F. von Groote-Bidlingmaier, C. M. Mendel, Efficiency and safety of the combination of moxifloxacin, pretomanid (PA-824), and pyrazinamide during the first 8 weeks of antituberculosis treatment: a phase 2b, open-label, partly randomised trial in patients with drug-susceptible or drug-resistant pulmonary tuberculosis. *Lancet* **385**, 1738-1747 (2015).
9. M. Matsumoto, H. Hashizume, T. Tomishige, M. Kawasaki, H. Tsubouchi, H. Sasaki, Y. Shimokawa, M. Komatsu, OPC-67683, a nitro-dihydro-imidazooxazole derivative with promising action against tuberculosis in vitro and in mice. *PLoS medicine* **3**, e466 (2006).
10. European Medicines Agency, Summary of the European public assessment report (EPAR) for Deltyba. Found at *http://www.ema.europa.eu/docs/en_GB/document_library/EPAR_-_Public_assessment_report/human/002552/WC500166234.pdf* (2013). Last accessed on 18 June 2018.
11. U. Manjunatha, H. I. Boshoff, C. E. Barry, The mechanism of action of PA-824: Novel insights from transcriptional profiling. *Commun Integr Biol* **2**, 215-218 (2009).
12. C. Greening, F. H. Ahmed, A. E. Mohamed, B. M. Lee, G. Pandey, A. C. Warden, C. Scott, J. G. Oakeshott, M. C. Taylor, C. J. Jackson, Physiology, Biochemistry, and Applications of F420- and Fo-Dependent Redox Reactions. *Microbiol Mol Biol Rev* **80**, 451-493 (2016).
13. S. E. Cellitti, J. Shaffer, D. H. Jones, T. Mukherjee, M. Gurumurthy, B. Bursulaya, H. I. Boshoff, I. Choi, A. Nayyar, Y. S. Lee, J. Cherian, P. Niyomrattanakit, T. Dick, U. H. Manjunatha, C. E. Barry, 3rd, G. Spraggon, B. H. Geierstanger, Structure of Ddn, the

deazaflavin-dependent nitroreductase from Mycobacterium tuberculosis involved in bioreductive activation of PA-824. *Structure* **20**, 101-112 (2012).

14. G. Bashiri, C. J. Squire, N. J. Moreland, E. N. Baker, Crystal structures of F420-dependent glucose-6-phosphate dehydrogenase FGD1 involved in the activation of the anti-tuberculosis drug candidate PA-824 reveal the basis of coenzyme and substrate binding. *The Journal of biological chemistry* **283**, 17531-17541 (2008).

15. D. E. Graham, H. Xu, R. H. White, Identification of the 7,8-didemethyl-8-hydroxy-5-deazariboflavin synthase required for coenzyme F(420) biosynthesis. *Arch Microbiol* **180**, 455-464 (2003).

16. K. P. Choi, T. B. Bair, Y. M. Bae, L. Daniels, Use of transposon Tn5367 mutagenesis and a nitroimidazopyran-based selection system to demonstrate a requirement for fbiA and fbiB in coenzyme F(420) biosynthesis by Mycobacterium bovis BCG. *J Bacteriol* **183**, 7058-7066 (2001).

17. L. Decamps, B. Philmus, A. Benjdia, R. White, T. P. Begley, O. Berteau, Biosynthesis of F0, precursor of the F420 cofactor, requires a unique two radical-SAM domain enzyme and tyrosine as substrate. *J Am Chem Soc* **134**, 18173-18176 (2012).

18. K. P. Choi, N. Kendrick, L. Daniels, Demonstration that fbiC is required by Mycobacterium bovis BCG for coenzyme F(420) and FO biosynthesis. *J Bacteriol* **184**, 2420-2428 (2002).

19. L. L. Grochowski, H. Xu, R. H. White, Identification and characterization of the 2-phospho-L-lactate guanylyltransferase involved in coenzyme F420 biosynthesis. *Biochemistry* **47**, 3033-3037 (2008).

20. D. Guerra-Lopez, L. Daniels, M. Rawat, Mycobacterium smegmatis mc2 155 fbiC and MSMEG_2392 are involved in triphenylmethane dye decolorization and coenzyme F420 biosynthesis. *Microbiology* **153**, 2724-2732 (2007).

21. C. K. Stover, P. Warrener, D. R. VanDevanter, D. R. Sherman, T. M. Arain, M. H. Langhorne, S. W. Anderson, J. A. Towell, Y. Yuan, D. N. McMurray, B. N. Kreiswirth, C. E. Barry, W. R. Baker, A small-molecule nitroimidazopyran drug candidate for the treatment of tuberculosis. *Nature* **405**, 962-966 (2000).

22. H. L. Haver, A. Chua, P. Ghode, S. B. Lakshminarayana, A. Singhal, B. Mathema, R. Wintjens, P. Bifani, Mutations in genes for the F420 biosynthetic pathway and a nitroreductase enzyme are the primary resistance determinants in spontaneous in vitro-selected PA-824-resistant mutants of Mycobacterium tuberculosis. *Antimicrobial agents and chemotherapy* **59**, 5316-5323 (2015).

23. M. Fujiwara, M. Kawasaki, N. Hariguchi, Y. Liu, M. Matsumoto, Mechanisms of resistance to delamanid, a drug for Mycobacterium tuberculosis. *Tuberculosis (Edinb)* **108**, 186-194 (2018).

24. S. Subbian, L. Tsenova, M. J. Kim, H. C. Wainwright, A. Visser, N. Bandyopadhyay, J. S. Bader, P. C. Karakousis, G. B. Murrmann, L. G. Bekker, D. G. Russell, G. Kaplan, Lesion-Specific Immune Response in Granulomas of Patients with Pulmonary Tuberculosis: A Pilot Study. *PLoS One* **10**, e0132249 (2015).

25. D. Rifat, B. Prideaux, R. M. Savic, M. E. Urbanowski, T. L. Parsons, B. Luna, M. A. Marzinke, A. A. Ordonez, V. P. DeMarco, S. K. Jain, V. Dartois, W. R. Bishai, K. E. Dooley, Pharmacokinetics of rifapentine and rifampin in a rabbit model of tuberculosis and correlation with clinical trial data. *Science translational medicine* **10**, (2018).

26. E. L. Nuermberger, T. Yoshimatsu, S. Tyagi, K. Williams, I. Rosenthal, R. J. O'Brien, A. A. Vernon, R. E. Chaisson, W. R. Bishai, J. H. Grosset, Moxifloxacin-containing regimens of reduced duration produce a stable cure in murine tuberculosis. *American journal of respiratory and critical care medicine* **170**, 1131-1134 (2004).

27. S. Tyagi, E. Nuermberger, T. Yoshimatsu, K. Williams, I. Rosenthal, N. Lounis, W. Bishai, J. Grosset, Bactericidal activity of the nitroimidazopyran PA-824 in a murine model of tuberculosis. *Antimicrobial agents and chemotherapy* **49**, 2289-2293 (2005).

28. M. H. Larsen, K. Biermann, S. Tandberg, T. Hsu, W. R. Jacobs, Jr., Genetic Manipulation of Mycobacterium tuberculosis. *Current protocols in microbiology* **Chapter 10**, Unit 10A 12 (2007).

29. T. R. Ioerger, Y. Feng, K. Ganesula, X. Chen, K. M. Dobos, S. Fortune, W. R. Jacobs, Jr., V. Mizrahi, T. Parish, E. Rubin, C. Sassetti, J. C. Sacchettini, Variation among genome sequences of H37Rv strains of Mycobacterium tuberculosis from multiple laboratories. *J Bacteriol* **192**, 3645-3653 (2010).

30. T. R. Ioerger, T. O'Malley, R. Liao, K. M. Guinn, M. J. Hickey, N. Mohaideen, K. C. Murphy, H. I. Boshoff, V. Mizrahi, E. J. Rubin, C. M. Sassetti, C. E. Barry, 3rd, D. R. Sherman, T. Parish, J. C. Sacchettini, Identification of new drug targets and resistance mechanisms in Mycobacterium tuberculosis. *PLoS One* **8**, e75245 (2013).

31. M. H. Lee, L. Pascopella, W. R. Jacobs, Jr., G. F. Hatfull, Site-specific integration of mycobacteriophage L5: integration-proficient vectors for Mycobacterium smegmatis, Mycobacterium tuberculosis, and bacille Calmette-Guerin. *Proceedings of the National Academy of Sciences of the United States of America* **88**, 3111-3115 (1991).

32. D. Rifat, D. A. Belchis, P. C. Karakousis, senX3-independent contribution of regX3 to Mycobacterium tuberculosis virulence. *BMC microbiology* **14**, 265 (2014).

33. D. Almeida, T. Ioerger, S. Tyagi, S. Y. Li, K. Mdluli, K. Andries, J. Grosset, J. Sacchettini, E. Nuermberger, Mutations in pepQ Confer Low-Level Resistance to Bedaquiline and Clofazimine in Mycobacterium tuberculosis. *Antimicrobial agents and chemotherapy* **60**, 4590-4599 (2016).

34. Z. Ahmad, C. A. Peloquin, R. P. Singh, H. Derendorf, S. Tyagi, A. Ginsberg, J. H. Grosset, E. L. Nuermberger, PA-824 exhibits time-dependent activity in a murine model of tuberculosis. *Antimicrobial agents and chemotherapy* **55**, 239-245 (2011).

35. G. Bashiri, A. M. Rehan, D. R. Greenwood, J. M. Dickson, E. N. Baker, Metabolic engineering of cofactor F420 production in Mycobacterium smegmatis. *PLoS One* **5**, 0015803 (2010).

36. D. Isabelle, D. R. Simpson, L. Daniels, Large-Scale Production of Coenzyme F(420)-5,6 by Using Mycobacterium smegmatis. *Applied and environmental microbiology* **68**, 5750-5755 (2002).

37. T. B. Bair, D. W. Isabelle, L. Daniels, Structures of coenzyme F(420) in Mycobacterium species. *Arch Microbiol* **176**, 37-43 (2001).

38. D. Rifat, P. C. Karakousis, Differential regulation of the two-component regulatory system senX3-regX3 in Mycobacterium tuberculosis. *Microbiology* **160**, 1125-1133 (2014).

39. R. Dawson, A. H. Diacon, D. Everitt, C. van Niekerk, P. R. Donald, D. A. Burger, R. Schall, M. Spigelman, A. Conradie, K. Eisenach, A. Venter, P. Ive, L. Page-Shipp, E. Variava, K. Reither, N. E. Ntinginya, A. Pym, F. von Groote-Bidlingmaier, C. M. Mendel, Efficiency and safety of the combination of moxifloxacin, pretomanid (PA-824), and pyrazinamide during the first 8 weeks of antituberculosis treatment: a phase 2b, open-label, partly randomised trial in patients with drug-susceptible or drug-resistant pulmonary tuberculosis. *Lancet* **385**, 1738-1747 (2015).

40. U. H. Manjunatha, H. Boshoff, C. S. Dowd, L. Zhang, T. J. Albert, J. E. Norton, L. Daniels, T. Dick, S. S. Pang, C. E. Barry, 3rd, Identification of a nitroimidazo-oxazine-specific protein involved in PA-824 resistance in Mycobacterium tuberculosis. *Proceedings of the National Academy of Sciences of the United States of America* **103**, 431-436 (2006).

41. WHO, Technical report on critical concentrations for TB drug susceptibility testing of medicines used in the treatment of drug-resistant TB. *http://www.who.int/tb/publications/2018/WHO_technical_report_concentrations_TB_drug_susceptibility,* (2018).

42. J. G. Hurdle, R. B. Lee, N. R. Budha, E. I. Carson, J. Qi, M. S. Scherman, S. H. Cho, M. R. McNeil, A. J. Lenaerts, S. G. Franzblau, B. Meibohm, R. E. Lee, A microbiological assessment of novel nitrofuranylamides as anti-tuberculosis agents. *J Antimicrob Chemother* **62**, 1037-1045 (2008).

43. G. V. Bloemberg, P. M. Keller, D. Stucki, A. Trauner, S. Borrell, T. Latshang, M. Coscolla, T. Rothe, R. Homke, C. Ritter, J. Feldmann, B. Schulthess, S. Gagneux, E. C. Bottger, *Acquired Resistance to Bedaquiline and Delamanid in Therapy for Tuberculosis*. (N Engl J Med. 2015 Nov 12;373(20):1986-8. doi: 10.1056/NEJMc1505196.).

44. K. Stinson, N. Kurepina, A. Venter, M. Fujiwara, M. Kawasaki, J. Timm, E. Shashkina, B. N. Kreiswirth, Y. Liu, M. Matsumoto, L. Geiter, MIC of Delamanid (OPC-67683) against Mycobacterium tuberculosis Clinical Isolates and a Proposed Critical Concentration. *Antimicrobial agents and chemotherapy* **60**, 3316-3322 (2016).

45. H. Hoffmann, T. A. Kohl, S. Hofmann-Thiel, M. Merker, P. Beckert, K. Jaton, L. Nedialkova, E. Sahalchyk, T. Rothe, P. M. Keller, S. Niemann, Delamanid and Bedaquiline Resistance in Mycobacterium tuberculosis Ancestral Beijing Genotype Causing Extensively Drug-Resistant Tuberculosis in a Tibetan Refugee. *American journal of respiratory and critical care medicine* **193**, 337-340 (2016).

46. J. Harper, C. Skerry, S. L. Davis, R. Tasneen, M. Weir, I. Kramnik, W. R. Bishai, M. G. Pomper, E. L. Nuermberger, S. K. Jain, Mouse model of necrotic tuberculosis granulomas develops hypoxic lesions. *The Journal of infectious diseases* **205**, 595-602 (2012).

47. E. Schena, L. Nedialkova, E. Borroni, S. Battaglia, A. M. Cabibbe, S. Niemann, C. Utpatel, M. Merker, A. Trovato, S. Hofmann-Thiel, H. Hoffmann, D. M. Cirillo, Delamanid susceptibility testing of Mycobacterium tuberculosis using the resazurin microtitre assay and the BACTEC MGIT 960 system. *J Antimicrob Chemother* **71**, 1532-1539 (2016).

48. S. Feuerriegel, C. U. Koser, D. Bau, S. Rusch-Gerdes, D. K. Summers, J. A. Archer, M. A. Marti-Renom, S. Niemann, Impact of Fgd1 and ddn diversity in Mycobacterium tuberculosis complex on in vitro susceptibility to PA-824. *Antimicrobial agents and chemotherapy* **55**, 5718-5722 (2011).

49. A. N. Yadon, K. Maharaj, J. H. Adamson, Y. P. Lai, J. C. Sacchettini, T. R. Ioerger, E. J. Rubin, A. S. Pym, A comprehensive characterization of PncA polymorphisms that confer resistance to pyrazinamide. *Nature communications* **8**, 588 (2017).

50. D. V. Cousins, B. R. Francis, B. L. Gow, Advantages of a new agar medium in the primary isolation of Mycobacterium bovis. *Veterinary microbiology* **20**, 89-95 (1989).

51. N. C. Mirabal, S. L. Yzquierdo, D. Lemus, M. Madruga, Y. Milian, M. Echemendia, H. Takiff, A. Martin, P. Van der Stuyf, J. C. Palomino, E. Montoro, Evaluation of colorimetric methods using nicotinamide for rapid detection of pyrazinamide resistance in Mycobacterium tuberculosis. *J Clin Microbiol* **48**, 2729-2733 (2010).

52. A. Y. Coban, M. Uzun, Rapid detection of multidrug-resistant Mycobacterium tuberculosis using the malachite green decolourisation assay. *Mem Inst Oswaldo Cruz* **108**, 1021-1023 (2013).

53. A. Martin, F. Portaels, J. C. Palomino, Colorimetric redox-indicator methods for the rapid detection of multidrug resistance in Mycobacterium tuberculosis: a systematic review and meta-analysis. *J Antimicrob Chemother* **59**, 175-183 (2007).

54. P. Farnia, F. Mohammadi, M. Mirsaedi, A. Z. Zarife, J. Tabatabee, K. Bahadori, M. Bahadori, M. R. Masjedi, A. A. Velayati, Application of oxidation-reduction assay for

monitoring treatment of patients with pulmonary tuberculosis. *J Clin Microbiol* **42**, 3324-3325 (2004).

55.　T. Jirapanjawat, B. Ney, M. C. Taylor, A. C. Warden, S. Afroze, R. J. Russell, B. M. Lee, C. J. Jackson, J. G. Oakeshott, G. Pandey, C. Greening, The redox cofactor F420 protects mycobacteria from diverse antimicrobial compounds and mediates a reductive detoxification system. *Applied and environmental microbiology*, (2016).

56.　M. S. Jang, Y. M. Lee, C. H. Kim, J. H. Lee, D. W. Kang, S. J. Kim, Y. C. Lee, Triphenylmethane reductase from Citrobacter sp. strain KCTC 18061P: purification, characterization, gene cloning, and overexpression of a functional protein in Escherichia coli. *Applied and environmental microbiology* **71**, 7955-7960 (2005).

57.　V. Fessard, T. Godard, S. Huet, A. Mourot, J. M. Poul, Mutagenicity of malachite green and leucomalachite green in in vitro tests. *J Appl Toxicol* **19**, 421-430 (1999).

58.　M. Gurumurthy, M. Rao, T. Mukherjee, S. P. Rao, H. I. Boshoff, T. Dick, C. E. Barry, 3rd, U. H. Manjunatha, A novel F(420) -dependent anti-oxidant mechanism protects Mycobacterium tuberculosis against oxidative stress and bactericidal agents. *Molecular microbiology* **87**, 744-755 (2013).

59.　K. H. Darwin, S. Ehrt, J. C. Gutierrez-Ramos, N. Weich, C. F. Nathan, The proteasome of Mycobacterium tuberculosis is required for resistance to nitric oxide. *Science* **302**, 1963-1966 (2003).

TABLES

Table 1. Mutations identified in 89 individual colonies and pooled isolates of pretomanid-resistant *M. tuberculosis* selected in BALB/c mice

Pretomanid treatment (mg/kg)	Mouse ID	No. of single isolates (n=89)	Gene name, amino acid (aa) length and no. of unique mutations selected (n=54)					
			Rv3261(fbiA) 331aa (n=7)	Rv3262(fbiB) 448aa (n=3)	Rv1173(fbiC) 856aa (n=29)	Rv3547(ddn) 151aa (n=5)	Rv0407(fgd1) 336aa (n=2)	Rv2983(cofC) 214aa (n=8)
0	M-1	2				-G in aa 38	K9N	
	M-2	4			R133P (2); -A in aa 503		K9N	
	M-4	1			W690*			
	M-5	4			+A in aa 426 (4)			
10	M-1	8	A212V		L702R (4); C562W	-GC in aa 39		+C in aa 27
	M-2	2			9 bp del (aa 307-309); -TCCCCGATG del in aa 306-308			
	M-3	4		L15P	L772W; -C in aa 252 (2)			
	M-4	5						G147C (5)
	M-5	2			A632V			R25G
30	M-1	1			S169P			
	M-2	3	L211P			W20*		A132V
	M-3	2			R278P (2)			
	M-4	1			W155*			
	M-5	3			Q400*; +T in aa 188 (2)			
100	M-1	1						-ATC in aa 129
	M-2	3			K682E; Y170*; L187R			
	M-3	2		W397R; L173P				
	M-4	2			F744S	-C in aa 93		
	M-5	4	S219G		M776T (3)			
300	M-1	7						R25S (7)
	M-2	4	Q27* (3); -G in aa 248					
	M-3	4			H190N; Q20*; -GC in aa 846 (2)			
	M-4	4			T707M; T301A; -C in aa 247	9345 bp del (Rv3540-Rv3550)		
	M-5	7	W79* (6)					A198P
600	M-1	1			N336K			
	M-2	5			R500* (5)			
	M-3	1	D49G					
	M-4	2						C152R (2)

Note: * : stop codon: + or ins: insertion; - or del: deletion; no. in parenthesis next to a mutation: no. of isolates with the same mutation.

Table 2. Mutations identified in 64 individual colonies and pooled isolates of nitrioimidazole-resistant *M. tuberculosis* selected in C3HeB/FeJ mice

Pretomanid treatment (mg/kg)	Mouse ID	No. of single isolates (n=64)	Gene name, amino acid (aa) length and no. of unique mutations selected (n=45)					
			Rv3261 (*fbiA*) 331aa (n=8)	*Rv3262* (*fbiB*) 448aa (n=1)	*Rv1173* (*fbiC*) 856aa (n=25)	*Rv3547* (*ddn*) 151aa (n=7)	*Rv0407* (*fgd1*) 336aa (n=2)	*Rv2983* (*cofC*) 214aa (n=2)
10	M-1	4			-A in aa 331;G194D; W198*			A68E
	M-2	4		-T in aa 353	-C in aa 363		+A in aa 214 (2)	
	M-3	2			-C in aa 20	L49P		
	M-4	2			K684T			Q114R
	M-5	1			del 42 bp (aa 680-693)			
30	M-1	5			-A in aa 225;+G in aa 107 (2)	W27*		
					IS6110 in 85bp upstream of *fbiC*			
	M-2	5	-GC in aa 140		L377P (2); L377P (2, het, p)			
	M-4	3			G148D; W354R	C149Y		
	M-5	3	G273D (2)		1 kb del (fbiC+PE12)			
100	M-1	5				IS6110 ins. in aa 131	G191D (5)	
	M-2	1			del 4 bp in aa 75-76			
	M-3	3	-G in aa 47 (2)		L685R			
	M-4	5	+C in aa 125		A588P (2): -G in aa 52; R322L			
	M-5	2	L308P (2)					
300	M-1	5			A591D (2); A827G; +C in aa 328 (2)			
	M-2	5	Q120P (3)		R322L; -T in aa 627			
	M-3	2	Q120P (2)					
	M-4	3				R112W (2); IS6110 ins. in D108		
	M-5	4	D286A		T273K (2)	-G in aa 39		

Note: * : stop codon: + or ins: insertion; - or del: deletion; no. in parenthesis next to a mutation: no. of isolates with the same mutation.

Table 3. Distribution of mutation types and frequencies in genes associated with pretomanid resistance, by mouse strain

Mouse model	Type of mutation	Gene name and amino acid (aa) length						No. of mutation	Frequency of mutation
		Rv3261 (*fbiA*) 331aa	*Rv3262* (*fbiB*) 448aa	*Rv1173* (*fbiC*) 856aa	*Rv3547* (*ddn*) 151aa	*Rv0407* (*fgd1*) 336aa	*Rv2983* (*cofC*) 214aa		
BALB/c	no. of point mutation	4	3	15	0	2	6	30	56%
	no. of indels (ins+del)	1	0	8	4	0	2	15	28%
	no. of stop codon	2	0	6	1	0	0	9	17%
	no. of total mutation	7	3	29	5	2	8	54	100%
	frequency of mutation	13%	6%	54%	9%	4%	15%	100%	
C3HeB/FeJ	no of point mutation	5	0	12	3	1	2	23	51%
	no of indels (ins+del)	3	1	12	3	1	0	20	44%
	no. of stop codon	0	0	1	1	0	0	2	4%
	no. of total mutation	8	1	25	7	2	2	45	100%
	frequency of mutation	18%	2%	56%	16%	4%	4%	100%	

Note: ins: insertion; del: deletion.

FIGURES
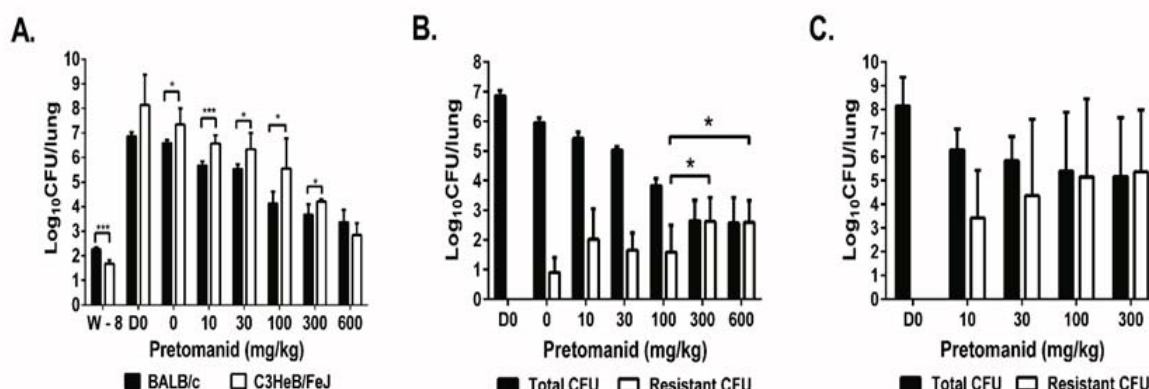
Fig. 1. Selective amplification of spontaneous pretomanid-resistant mutants during pretomanid monotherapy in mice is dose-dependent and is more pronounced in C3HeB/FeJ mice. After aerosol infection with *M. tuberculosis* H37Rv, BALB/c and C3HeB/FeJ mice were treated with a range of doses of pretomanid for 8 weeks and sacrificed at different time points before and after treatment for lung CFU counts. A. Mean (± S.D.) total lung CFU counts on the day after infection (W-8), on the day of treatment initiation (D0), and after 3 weeks of treatment with the indicated pretomanid dose (in mg/kg body weight). Dose-dependent bactericidal activity was observed in both strains; B. Mean (± S.D.) total and PMD-resistant lung CFU counts in BALB/c mice on day 0 and after 8 weeks of treatment with the indicated pretomanid dose. Dose-dependent bactericidal activity and selection of PMD-resistant bacteria was observed, with the resistant population overtaking the susceptible population at doses ≥ 300 mg/kg; C. Mean (± S.D.) total and PMD-resistant lung CFU counts in C3HeB/FeJ mice on day 0 and after 8 weeks of treatment with the indicated pretomanid dose. Dose-dependent bactericidal activity and selection of PMD-resistant bacteria was observed, with the resistant population overtaking the susceptible population at doses ≥ 30 mg/kg. * $p < 0.05$, *** $p < 0.001$
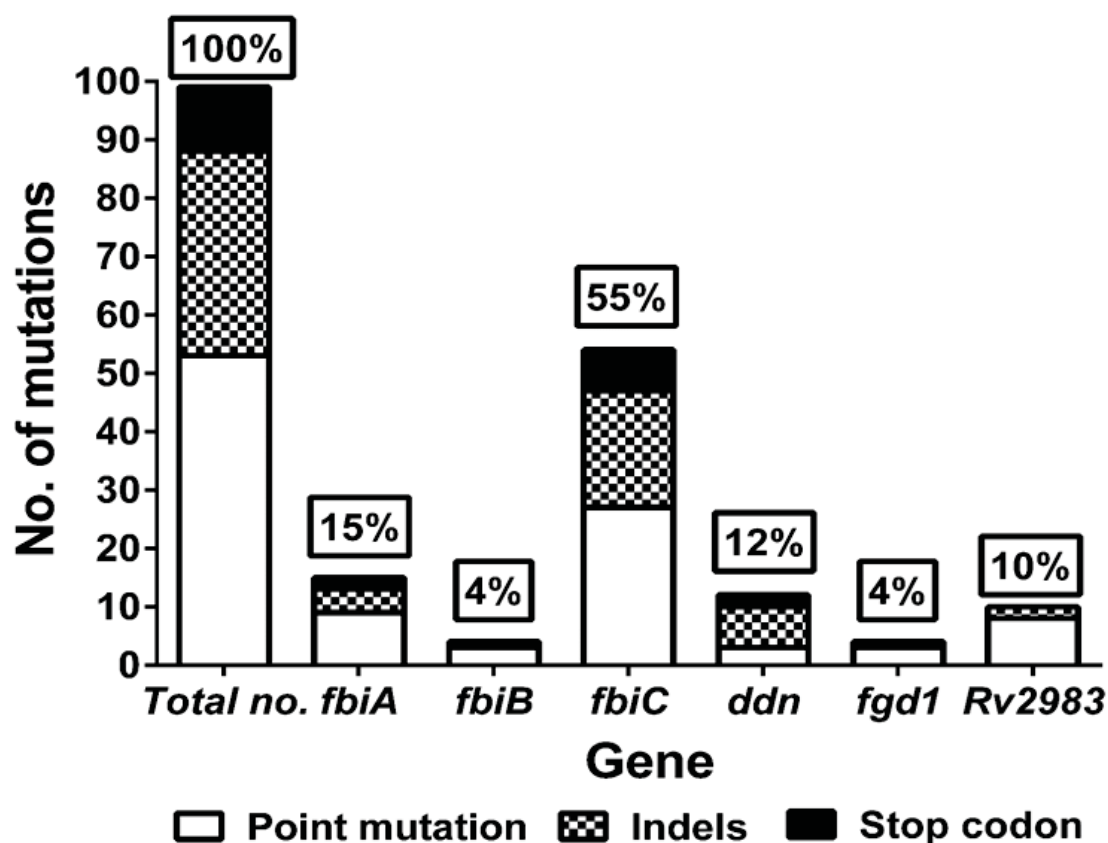
Fig. 2. Overall mutation frequencies of genes associated with pretomanid resistance. WGS was performed with 136 pretomanid-resistant colonies and 25 colony pools picked from 47 individual mice harboring pretomanid-resistant CFU after 8 weeks of treatment and identified 99 unique mutations in these 6 genes. Mutations in *fbiC* (55%) were the predominant cause of pretomanid resistance. For the other 5 genes, the rank order by mutation frequency was *fbiA* (15%), *ddn* (12%), *Rv2983* (10%), *fgd1* (4%) and *fbiB* (4%).
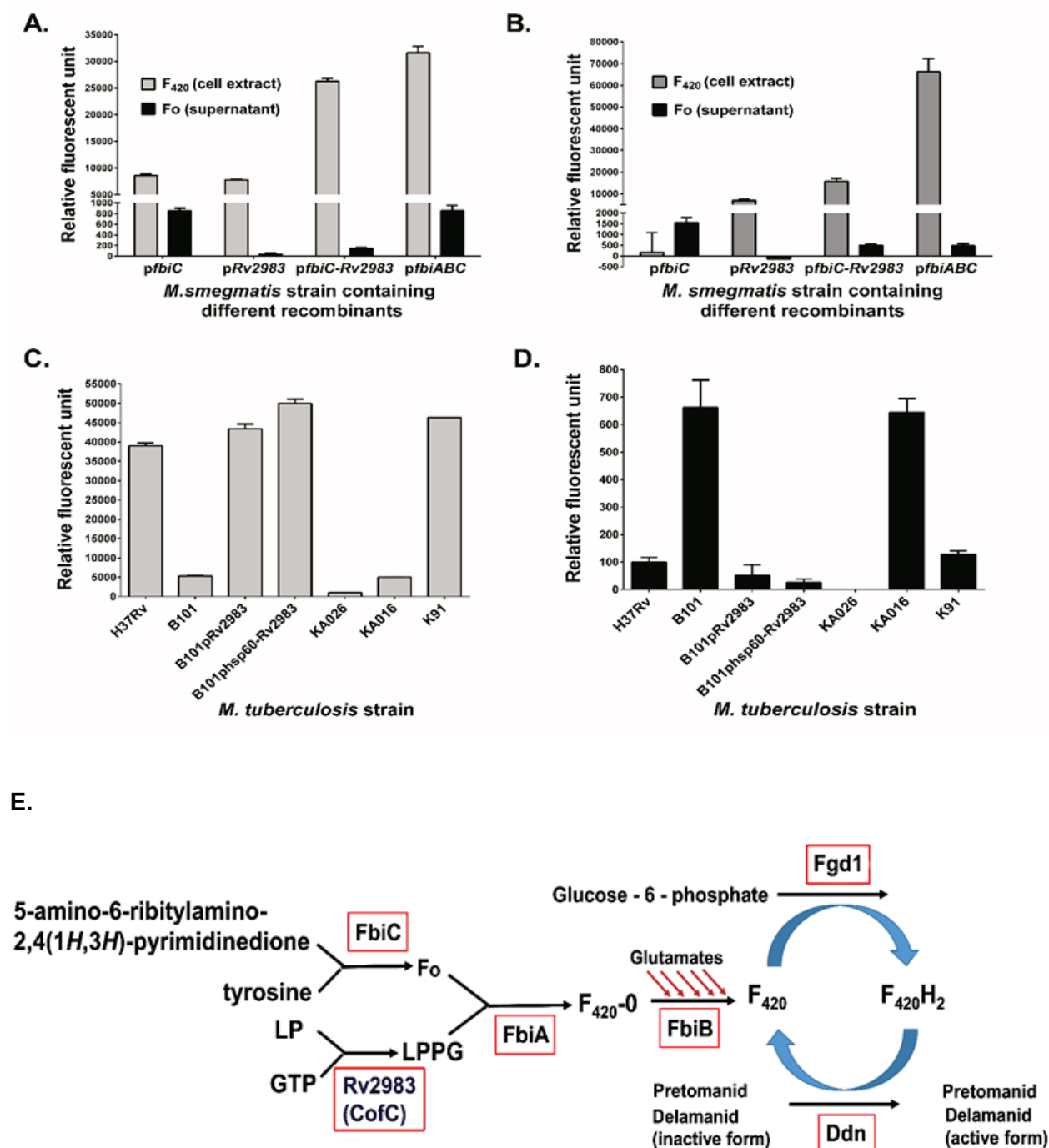
Fig. 3. Rv2983 is required for efficient F$_{420}$ synthesis from Fo. F$_{420}$ and Fo content was measured in *M. smegmatis* strains harboring different recombinants relative to the control strain containing the empty vector pYUBDuet after 6 (A) and 26 (B) hours of 1mM IPTG induction; F$_{420}$ (C) and Fo (D) content was measured in *Rv2983* mutant strains of *M. tuberculosis* and control

36

strains including B101 (ΔRv2983, A198P), KA016 (ΔRv2983, Q114R), H37Rv (wild-type), B101 complemented strain (pMH94-Rv2983), B101 complemented strain (pMH94-hsp60-Rv2983), KA026 (ΔfbiC, IS6110 insertion in 85-bp upstream of fbiC), and K91 (Δddn, IS6110 insertion in aa D108), after growth in 7H9 broth for 6 days. Schematic diagram (E) of proposed nitroimidazole activation pathway showing Rv2983 as putative CofC catalyzing LPPG biosynthesis. Fo, 7,8-didemethyl-8-hydroxy-5-deazariboflavin; LP, 2-phospho-L-lactate; GTP, guanosine triphosphate; LPPG, L-lactyl-2-diphospho-5'-guanosine.
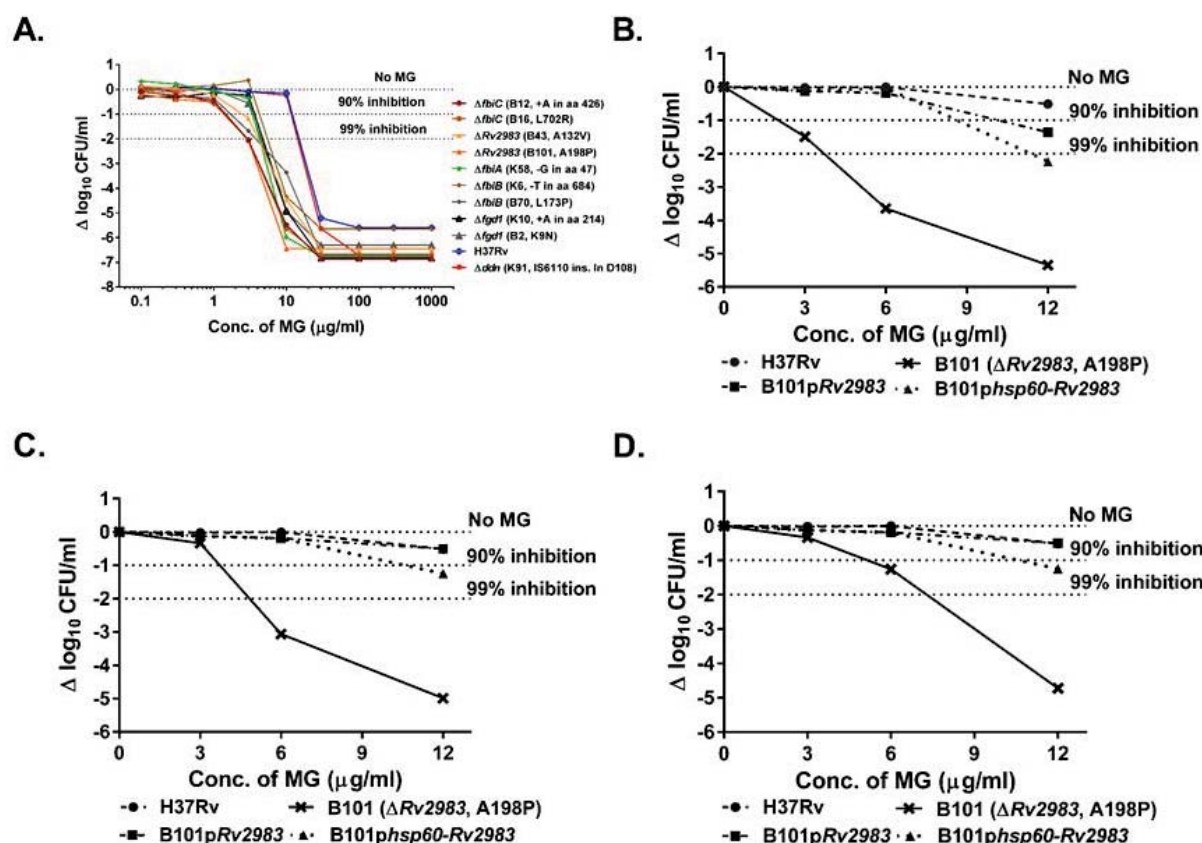
Fig. 4. $F_{420}H_2$-deficient pretomanid-resistant mutants of *M. tuberculosis* are more susceptible to growth inhibition by malachite green. A. Growth of wild-type *M. tuberculosis* on 7H9 agar is inhibited by malachite green (MG) in a concentration-dependent manner. $F_{420}H_2$-deficient, pretomanid-resistant *M. tuberculosis* mutants (*fbiA-C, fgd1, Rv2983*) are inhibited at lower MG concentrations relative to the wild type and the $F_{420}H_2$-sufficient, pretomanid-resistant *ddn* mutant. B-D. Complementation of the B101 mutant with wild-type *Rv2983* restores tolerance to MG and the proportional recovery of the mutant on 6 µg/ml of MG increases as the duration of incubation increases from 28 (B), to 35 (C) to 49 (D) days of incubation. The proportional recovery of the mutant on plates containing 12 µg/ml of MG does not increase with time.
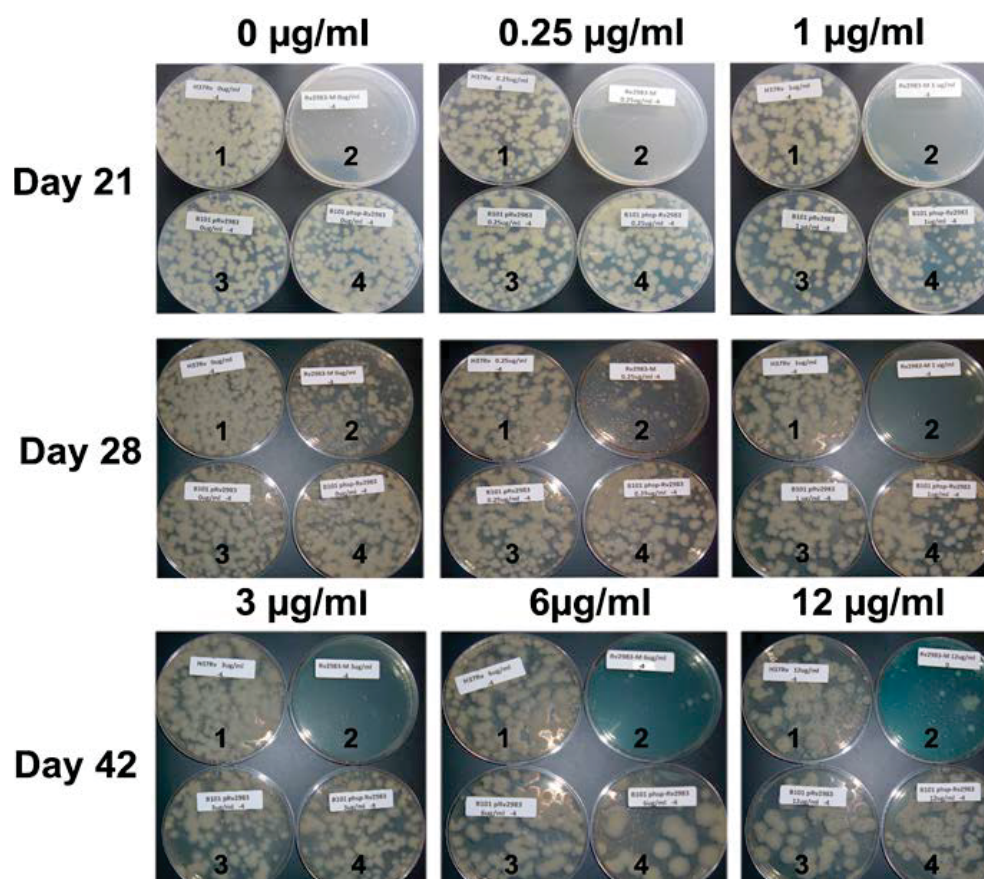
Fig. 5. Mutation of *Rv2983* causes growth inhibition and defective decolorization of malachite green. Aliquots (100 µl) of *M. tuberculosis* cultures (1, H37Rv wild type; 2, *Rv2983* mutant B101; 3, B101 mutant complemented with *Rv2983* behind native promoter; 4, B101 mutant complemented with *Rv2983* behind *hsp60* promoter) were spread on 7H9 agar plates containing increasing concentrations of malachite green (MG) after serial 10-fold dilutions. Colony size and MG decolorization are depicted after different incubation times. Numbers on plate labels (e.g., 0, 3, 4, 5) indicate the number of 10-fold dilutions performed before an aliquot was plated. Although the B101 mutant grows more slowly on plates without MG, growth is further slowed in the presence of ≥0.25 µg/ml of MG and the proportion of CFU recovered declines with increasing MG concentrations above 0.25 µg/ml. For plates containing 6 and 12 µg/ml of MG, plates receiving more-concentrated aliquots of the B101 mutant culture are shown to demonstrate the markedly reduced recovery of the mutant at these MG concentrations.

39
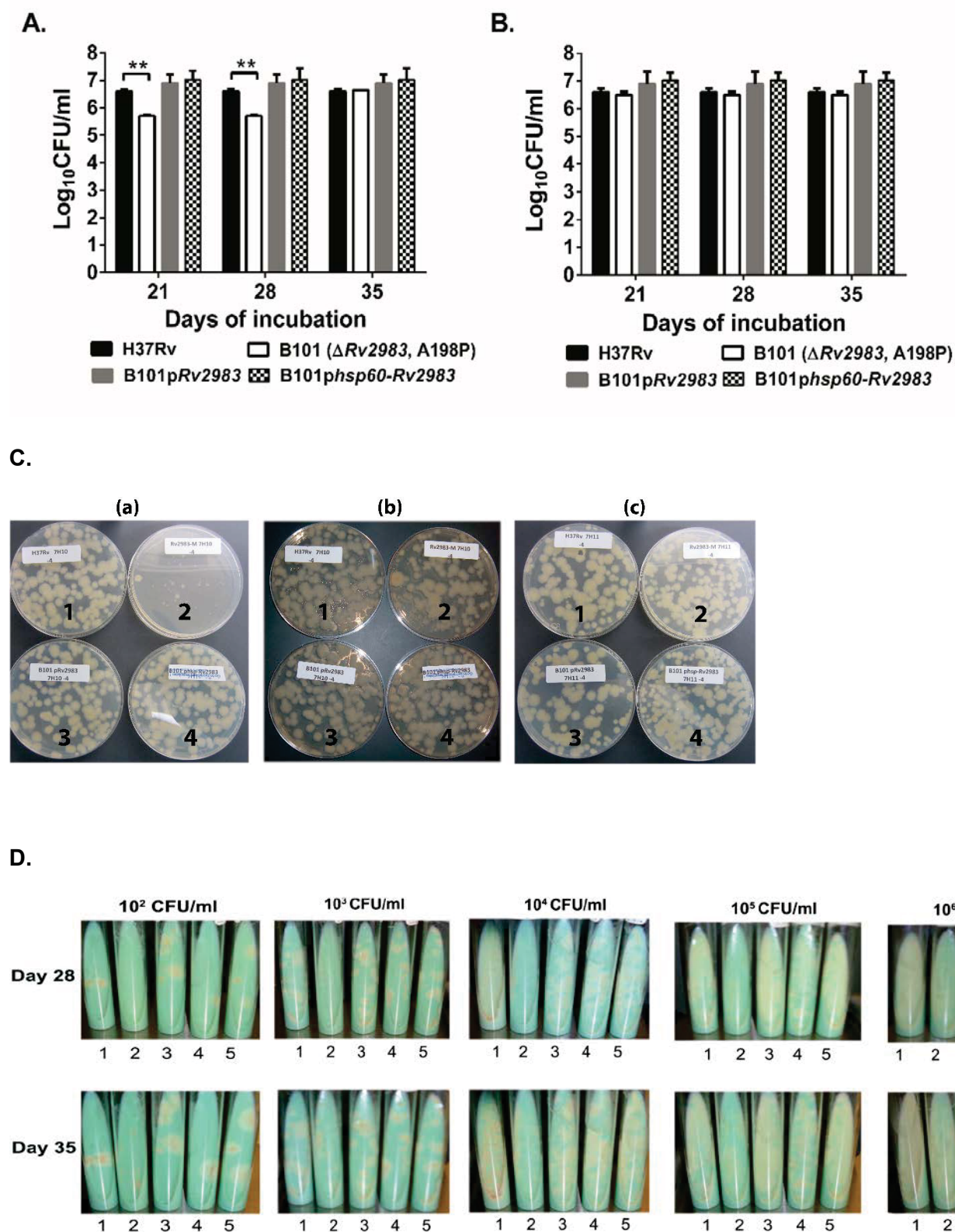
Fig. 6. Mutation of *Rv2983* causes growth inhibition on commercial 7H10 agar and LJ slants, but not on commercial 7H11 agar. Aliquots of *M. tuberculosis* cultures were spread on various solid media purchased commercially after serial 10-fold dilutions. A-B. Mean CFU counts on 7H10 (A) and 7H11 (B) agar plates; C. Colonies on 7H10 agar plates after 21 (a) and 35 (b) days of incubation, and on 7H11 agar plates after 21 (c) days of incubation; D. Colonies on LJ slants inoculated with serially diluted aliquots after 28 and 35 days of incubation. 1: H37Rv wild type; 2: B101 mutant (Δ*Rv2983*, A198P); 3: B101 mutant complemented with *Rv2983* behind the native promoter; 4: B101 mutant complemented with *Rv2983* behind the *hsp60* promoter; 5. K91 mutant (Δ*ddn*, IS6110 ins in D108).

.

SUPPLEMENTARY MATERIALS

Table S1. List of the primers used in the study

Table S2. WGS results for 136 individual pretomanid-resistant colonies selected with different

doses of pretomanid in *M. tuberculosis*-infected BALB/c and C3HeB/FeJ mice

Table S3. WGS results for 25 pooled pretomanid-resistant isolates selected with different doses

of pretomanid in *M. tuberculosis*-infected BALB/c and C3HeB/FeJ mice

Table S4. Distribution of overall mutation types and frequencies in genes associated with

pretomanid resistance

Table S5. Pretomanid MICs against selected pretomanid-resistant *M. tuberculosis* mutants

Figure S1. Complementation of B101 mutant with *Rv2983*. A. Schematic diagram of genomic

DNA of *M. tuberculosis* strains after digestion with restriction enzyme Acc65I; B. Result of

southern blot confirmed expected DNA fragments after Acc65I digestion using DIG-labeled

Rv2983 probe (H37Rv: 6.3 kb; Rv2983 mutant: 6.3 kb; complemented strains: 6.3 and 3.5 kb).

Figure S2. Expression of *Rv2983* and other genes involved in nitroimidazole activation. A.

Expression of *Rv2983* and other genes involved in nitroimidazole activation is higher in the

Rv2983 mutant B101 relative to the wild-type H37Rv after 4 days of incubation in 7H9 broth; B.

fbiC expression is dramatically lower in the *fbiC* mutant KA026 relative to the wild-type after 2

days of incubation in 7H9 broth; C. A faint band representing the 937-bp *fbiC* DNA fragment is

evident in the sample from the KA026 mutant (lane 2) relative to that in H37Rv (lane 3). Lane 1

is the 1-kb DNA marker.

Figure S3. Complementation of the B101 mutant with wild-type *Rv2983* restores tolerance to MG.

The proportional recovery of the mutant on 6 μg/ml of MG increases with the volume of culture

plated and the duration of incubation: 28-day incubation of 500 μl (A) aliquots/plate; 35-day

incubation of 500 μl (B) aliquots/plate.

42

SUPPLEMENTARY MATERIALS

Table S1. List of the primers used in the study

Primer name	Primer sequence	Purpose of amplification
Rv2983-1F	GCTCGGTACCCGGGGATCCTCCCAAGTGCCTCCTCGGC	*Rv2983* OFR and flanking sequences
Rv2983-1R	GGTGCCCTTGGTGGTCGACTGTTCGCCGTTGGTCTGCC	
hsp60- F	GCTCGGTACCCGGGGATCCTTCGGCCATGACAAGAATCTG	*hsp60* promoter
hsp60- R	TGCCGCTCATGCATGTTTGGGCGCATCC	
Rv2983- 2F	CCAAACATGCATGAGCGGCACACCGGAC	*Rv2983* ORF
Rv2983- 2R	GGTGCCCTTGGTGGTCGACTTCAACGATGTGCGACCGC	
Rv2983- 3F	GACTCGCGAGAACGTGGT	*Rv2983* DNA probe
Rv2983- 3R	CCAGGCTCCTGTCAGCTC	
Rv2983- 4F	GTATAAGAAGGAGATATACAATGAGCGGCACACCGGAC	*Rv2983* ORF
Rv2983- 4R	TGGCAGCAGCCTAGGTTAATTCAACGATGTGCGACCGC	
Rv2983-RT-F	CGATTTGCCGGCATTACAGA	expression of *Rv2983*
Rv2983-RT-R	CGAACGCACACAGTACCG	
fbiC-RT-F	GTCCATTCCGTTTACCACCG	expression of *fbiC*
fbiC-RT-R	CGGAAGTTCTGCACGATCAC	
fbiA-RT-1F	CCAGTTTGCTGCCAATTCTG	expression of *fbiA*
fbiA-RT-1R	ACATGCAGGTGTCCAGATCC	
fbiB-RT-F	GGATGAAAGACAAGTGGCGG	expression of *fbiB*
fbiB-RT-R	ACTTCGGGTGCGTCATAGAG	
fgd1-RT-F	GTACCCGAACCGTGTTTTCC	expression of *fgd1*
fgd1-RT-R	CATTAGCCCCACCGATTCAC	
sigA- F	CTACGCTACGTGGTGGATTC	expression of *sigA*
sigA-R	GGTGATGTCCATGTCTTTGG	
fbiC-5-7_F	GCAAGGTGTTTATCCCGGTC	*fbiC* DNA fragment
fbiC-5-7_R	TGTACGTATTTGGGTTGCGC	

Table S2. WGS results for 136 individual pretomanid-resistant colonies selected with different doses of pretomanid in *M. tuberculosis*-infected BALB/c and C3HeB/FeJ mice

43

Mouse model	Pretomanid treatment dose (mg/kg)	Mouse ID	Pretomanid selection concentration (µg/ml)	Name of isolates	Sample ID (DNA)	Sequencing coverage	Rv3261 (fbiA) 331aa (n=24, 17.6%)	Rv3262 (fbiB) 448aa (n=4, 2.9%)	Rv1173 (fbiC) 856aa (n=77, 56.6%)	Rv3547 (ddn) 151aa (n=9, 6.6%)	Rv0407 (fgd1) 336aa (n=5, 3.7%)	Rv2983 (cofC) 214aa (n=17, 12.5%)	Other mutations
BALB/c	0	M-1	0.25	BA_002	1963	37.2						K9N	
			1	BA_003	1964	37.9				-G in aa 38			NuoM:P26S
		M-2	0.25	BA_004	1965	35.1			-A in aa 503				PPE31:S12L; gabT:L361V
			0.25	BA_005	1966	39.6			R133P				
			0.25	BA_006	1967	32.7			R133P				
			10	BA_007	1968	57.7					K9N		
		M-4	1	BA_009	1969	46.5			W690*				
		M-5	0.25	BA_010	1970	27			+A in aa 426				
			1	BA_011	1971	49.2			+A in aa 426				
			10	BA_012	1972	49.5			+A in aa 426				
			10	BA_013	1973	39.2			+A in aa 426				
	10	M-1	0.25	BA_014	1974	41.6			L702R				
			0.25	BA_015	1975	54.9			L702R				
			1	BA_016	1976	45.6			L702R				
			10	BA_017	1977	40.5			C562W				
			10	BA_018a	1978	42			L702R				
			10	BA_019a	1979	28.5						+C in aa 27	citA:R293R; cya:V141F; Rv3541c:V108V; Rv3689:Q425R
		M-2	0.25	BA_020	1980	56.8			9 bp del (aa 307-309)				
			0.25	BA_021	1981	43.7				-GC in aa 39			
			1	BA_022	1982	53.6	A212V						nc230580:G>A
			10	BA_024	1984	76			-TCCCCGATG, del aa 306-308				
		M-3	0.25	BA_025	1985	93.9			-C in aa 252				fadD24:A364A
			0.25	BA_026a	1986	87.1		L15P					Rv1230c:C360G; trpA:Y35C; cycA:T433A; hflx:L435P
			10	BA_028	1988	59			-C in aa 252				fadD24:A364A
			10	BA_029	1989	49.5			L772W				Rv3254:A225S; Rv3805c:A417A
		M-4	1	BA_031	1991	93.9						G147C	Rv3254:A225S; Rv3805c:A417A
			1	BA_032	1992	83.7						G147C	Rv3254:A225S; Rv3805c:A417A
			10	BA_033	1993	114.2						G147C	Rv3254:A225S; Rv3805c:A417A
		M-5	0.25	BA_035	1995	80			A632V				fprB:V58F; secD:T232S
			1	BA_036	1996	47.8						R25G	
	30	M-1	10	BA_041	2001	28.3			S169P				Rv3792:V600F
		M-2	0.25	BA_043	2003	50.8						A132V	
			1	BA_044	2004	44.9				W20*			Rv1230c:C360G; trpA:Y35C; cycA:T433A
			10	BA_045	2005	47.9	L211P						ppsB:A354S
		M-3	1	BA_048	2008	37.9			R278P				Rv1129c:Y301Y; Rv1314c:P80P
			1	BA_049a	2009	69.3			R278P				Rv1129c:Y301Y; Rv1314c:P80P
		M-4	10	BA_053	2013	49			W155*				Rv3792:V600F
		M-5	0.25	BA_055	2015	66.5			Q400*				Rv1230c:C360G; nc3134222:C>T (41 bp downstream from Rv2825c)
			10	BA_058	2017	77.8			+T in aa 188				Rv1871c:G48D
			10	BA_059	2018	60.7			+T in aa 188				Rv1871c:G48D
	100	M-1	0.25	BA_060	2019	65.8					-ATC in aa 129		Rv3792:V600F
		M-2	0.25	BA_062	2021	75.6			K682E				Rv1230c:C360G
			10	BA_064	2023	72.4			Y170*				Rv1931c:A172A
			10	BA_065	2024	56.5			L187R				Rv0609c:G64S; rc789981:GG>AC; Rv2969c:S132A
		M-3	10	BA_069	2028	66.5		W397R					Rv3254:A225S; Rv3805c:A417A
			10	BA_070	2029	75.2		L173P					mprB:A491A; nadD:P332S; nc2639032:C>T (24bp downstream from PPE40)
		M-4	1	BA_071	2030	74.9			F744S				
			10	BA_072	2031	61.2				-C in aa 93			
		M-5	0.25	BA_074a	2033	69.6	S219G						bioF2:C450F
			1	BA_075	2034	67.4			M776T				fadD24:A364A; Rv1749c:W171R
			10	BA_076	2035	59.7			M776T				fadD24:A364A; Rv1749c:W171R
			10	BA_077	2036	64.3			M776T				fadD24:A364A; Rv1749c:W171R
	300	M-1	1	BA_078	2037	55						R25S	NarK3:A338A
			1	BA_079	2038	76.8						R25S	NarK3:A338A
			1	BA_080	2039	92.3						R25S	NarK3:A338A
			10	BA_081a	2040	125.5						R25S	NarK3:A338A
			10	BA_082	2041	86.9						R25S	NarK3:A338A
		M-2	1	BA_084	2043	77.5	Q27*						Rv0312:P510A, citA:R293R, Rv3541c:V108V, plus 3 other heterogeneous sites
			10	BA_086a	2045	62.3	-G in aa 248						Rv0102:Y176Y; Rv0579:L142P; Rv1230c:C360G
			10	BA_087	2046	49.1	Q27*						Rv0312:P510A; citA:R293R; Rv3541c:V108V
		M-3	0.25	BA_089	2048	78.3			H190N				nc3383560:G>A
			1	BA_090	2049	75.9			-GC in aa 846				
			10	BA_091	2050	56.3			-GC in aa 846				
			10	BA_092	2051	85.2			Q20*				fadE4:K33R(het)
		M-4	0.25	BA_093	2052	85.3			T707M				
			1	BA_095	2054	45.1				9345 bp del (Rv3540-Rv3550)			Rv2993c:P56Q
			10	BA_096	2055	84.3			T301A				Rv2993c:P56Q
			10	BA_097	2056	97.7			-C in aa 247				nc4020443:C>A (2bp downstream. of lppH)
		M-5	0.25	BA_098	2057	100.8	W79*						
			0.25	BA_099	2058	77	W79*						
			0.25	BA_100	2059	112.9	W79*						
			1	BA_101	2060	76.2						A198P	
			1	BA_102	2061	57.9	W79*						
	600	M-1	1	BA_103	2062	43.8			N336K				
		M-2	0.25	BA_106a	2063	100.8			R500*				pks7:V338L; lipN:C976G; lipN:I96R
			0.25	BA_107	2064	78.6			R500*				pks7:V338L; lipN:C976G; lipN:I96R
			1	BA_108	2065	60.9			R500*				pks7:V338L; lipN:C976G; lipN:I96R
			10	BA_109	2066	81.8			R500*				pks7:V338L; lipN:C976G; lipN:I96R
			10	BA_110	2067	90.2			R500*				pks7:V338L; lipN:C976G; lipN:I96R
		M-3	10	BA_114	2071	63.5	D49G						
		M-4	10	BA_119	2076	47.7						C152R	Rv3090:S254S
			10	BA_120	2077	76.1						C152R	Rv3090:S254S
C3HeB/FeJ	10	M-1	1	KA_001	1873	32.3			-A in aa 331				nrp:V1705A, pknD:T633N
			1	KA_003	1875	27.6					A68E		atpH:A439E;Rv2009:E12D
			10	KA_004	1876	23.1			G194D				
			10	KA_005	1877	42.2			W198*				
		M-2	1	KA_006	1878	39.2		-T in aa 353					nirB:V29A, xseA:V202V, nc3382560:G>A, Rv3242c:L73R
			1	KA_008	1879	87.2					+A in aa 214		
			10	KA_009	1880	58.8			-C in aa 363				lpqM:G3G
			10	KA_010	1881	84.7					+A in aa 214		
		M-3	10	KA_014	1885	29.8			-C in aa 20				
		M-4	0.25	KA_016	1887	94						Q114R	Rv0686:T90A; Rv3792:V600F
			1	KA_017	1888	81.8			K684T				fadD7:L103V; Rv1347c:F143L
		M-5	0.25	KA_022	1892	91.1			del 42 bp (aa 680-693)				nc3382560:G>A
	30	M-1	1	KA_026a	1896	41.9			IS6110 in 85bp upstream of fbiC				Rv0628c:A310S; Rv1975:A170S
			1	KA_028	1898	57.3			-A in aa 225				nadB:P332S
			10	KA_029	1899	36.5			+G in aa 107				
			10	KA_030	1900	43.6			+G in aa 107				
		M-2	1	KA_031	1901	40.6			L377P				R3831:P23P
			1	KA_032	1902	88.5			L377P				R3831:P23P
			10	KA_034	1904	33.1	-GC in aa 140						R3831:P23P
		M-4	0.25	KA_037	1907	85.9			G148D				Rv1230c:C360G; lipB:D101E
			1	KA_039	1909	82.2			W354R				Rv1230c:C360G
		M-5	0.25	KA_041	1911	103.7			1 kb del (fbiC+PE12)				
			0.25	KA_043	1913	122.8	G273D						lppN:L9F; Rv0669c:Q537R(53%)
			1	KA_044	1914	42.1	G273D						lppN:L9F
	100	M-1	1	KA_047	1916	34.8				IS6110 ins. in aa 131			cobN:M1045I
			10	KA_050	1919	83.3						G191D	
		M-2	0.25	KA_052	1921	94.9			del 4 bp in aa 75-76				ctpE:A448A; Rv1685c:T188N
		M-3	1	KA_057	1926	40.3			L685R				pta:L406R; uvrD1:D273D
			1	KA_058	1927	33.4			-G in aa 47				
			10	KA_059	1928	107.8			-G in aa 47				
		M-4	0.25	KA_061	1930	31.5			A588P				mca:T113A
			0.25	KA_062	1931	94.5			-G in aa 52				alkB:Y391D
			1	KA_063	1932	37.8			R322L				pks7:V338L; Rv3312A:D67H
			10	KA_064	1933	35.4	+C in aa 125						mca:T113A
			10	KA_065	1934	93.2			A588P				mca:T113A;Rv2817c:A280A
		M-5	10	KA_067	1935	42.2			L308P				Rv0609A:G64S; nc789981:GG>AC 45 bp downstream from Rv0690c; Rv2969c:S132A
			10	KA_068	1936	97.4			L308P				Rv0609c:G64S; nc789981:GG>AC; Rv2969c:S132A
	300	M-1	0.25	KA_071	1939	40.6			A591D				xseA:D388E
			0.25	KA_072	1940	96.2			+C in aa 328				pknI:L455R
			0.25	KA_073	1941	45.5			A827G				
			1	KA_074	1942	53.4			A591D				xseA:D388E
			1	KA_075	1943	45.7			+C in aa 328				pknI:L455R
		M-2	0.25	KA_076	1944	102.8			R322L				pks7:V338L; Rv3312A:D67H
			1	KA_078	1946	75.1			-T in aa 627				
			1	KA_079	1947	69.2	Q120P						acrA1:R161C; -G in PPE13 (9 aa from C-term); Rv3168:A182T
			10	KA_080	1948	73.8	Q120P						-G in PPE13 (9 aa from C-term)
			10	KA_081	1949	211.2	Q120P						Rv0285/PE5:V63G
		M-3	10	KA_085	1951	111.4	Q120P						acrA1:R161C; -G in PPE13 (9 aa from C-term)
		M-4	0.25	KA_088a	1953	41.5				R112W			
			1	KA_091	1955	63				IS6110 ins. in D108			
		M-5	1	KA_093	1957	194.5				-G in aa 39			nuoM:P26S
			1	KA_094	1958	44			T273K				Rv2842c:V153V
			10	KA_095	1959	119.4			T273K				Rv2842c:V153V
			10	KA_096	1960	119.7	D286A						Rv3867:D47N

Note: aa: amino acid; n: number of isolate and isolation rate among all the individual isolates; * : stop codon; +: insertion; -: deletion; ins: insertion; del: deletion; unknown: no mutation found in the six genes; >: substitution.

Table S3. WGS results for 25 pooled pretomanid-resistant isolates selected with different doses of pretomanid in *M. tuberculosis*-infected BALB/c and C3HeB/FeJ mice

Mouse model	Pretomanid treatment dose (mg/kg)	Mouse ID	Pretomanid selection concentration (µg/ml)	Name of pooled isolates	Sample ID (DNA)	Sequencing coverage	Rv3261(fbiA) 331aa	Rv3262(fbiB) 448aa	Rv1173(fbiC) 856aa	Rv3547(ddn) 151aa	Rv0407(fgd1) 336aa	Rv2983(cofC) 214aa	Other mutations
Balbc	10	M-4	1	P1	2084	103.4						G147C	Rv3254:A225S; Rv3805c:A417A
			10	P2	2085	140.3						G147C	Rv3254:A225S; Rv3805c:A417A
	300	M-1	1	P3	2086	123.1						R25S	narK3:A338A(het)
			10	P4	2087	74.5						R25S(het)	narK3:A338A(het)
		M-2	10	P6	2089	44.6	Q27*(het)						Rv3541c:V108V; Rv0312:P510A(het); citA:R293R(het)
		M-5	0.25	P7	2090	44.6	W79*						
			1	P8	2091	67.8	W79*						
	600	M-5	1	P9	2092	55.3							Rv2310:E94A; Rv3792:V600F(het); proS:A524E(het)
C3HeB/FeJ	10	M-1	10	P11	2094	39.5							nrp:V1705A; pknD:T633N
		M-3	1	P12	2095	34.4				L49P(het)			
	30	M-1	1	P13	2096	65.9				W27*(het)			Rv0628c:A310S(het); Rv1975:A170S(het)
			10	P14	2097	66.2							Rv0628c:A310S(het); Rv1975:A170S(het)
		M-2	1	P15	2098	35.5			L377P(het)				Rv3831:P23P
			10	P16	2099	53.1			L377P(het)				Rv3831:P23P
		M-4	0.25	P17	2100	53				C149Y(het)			Rv1230c:C360G(het); ureG:L58L(het); Rv2567:A728A(het); Rv3229c:T133A(het); nadB:P322S(het); Rv3447c:het
			1	P18	2101	67.7							Rv1230c:C360G(het); ureG:L58L(het); Rv2567:A728A(het); Rv3229c:T133A(het);nadB:P322S(het)
	100	M-1	0.25	P19	2102	73					G191D(het)		cobN:M1045I(het); groEL:G171G(het)
			1	P20	2103	33.8					G191D(het)		cobN:M1045I(het); groEL:G171G(het); Rv0987:indel?
			10	P21	2104	75					G191D(het)		groEL:G171G(het)
		M-4	1	P24	2107	48.6							
	300	M-1	1	P26	2108	44.4							pknI:L455R(het)
		M-3	1	P27	2109	30.8	Q120P(het)						
		M-4	0.25	P28	2110	93.4				R112W(het)			
			1	P29	2111	142.9							
		M-5	10	P31	2113	139.5							
Note: * : stop codon; het: heterogeneous.													

Table S4. Distribution of overall mutation types and frequencies in genes associated with pretomanid resistance

Type of mutation	Gene name and amino acid (aa) length						No. of mutation	Frequency of mutation
	Rv3261(fbiA) 331aa	Rv3262(fbiB) 448aa	Rv1173(fbiC) 856aa	Rv3547(ddn) 151aa	Rv0407(fgd1) 336aa	Rv2983(cofC) 214aa		
no. of point mutation	9	3	27	3	3	8	53	54%
no. of indels (ins+del)	4	1	20	7	1	2	35	35%
no. of stop codon	2	0	7	2	0	0	11	11%
no. of total mutation	15	4	54	12	4	10	99	100%
frequency of mutation	15%	4%	55%	12%	4%	10%	100%	
Note: ins: insertion; del: deletion.								

Table S5. Pretomanid MICs against selected pretomanid-resistant *M. tuberculosis* mutants

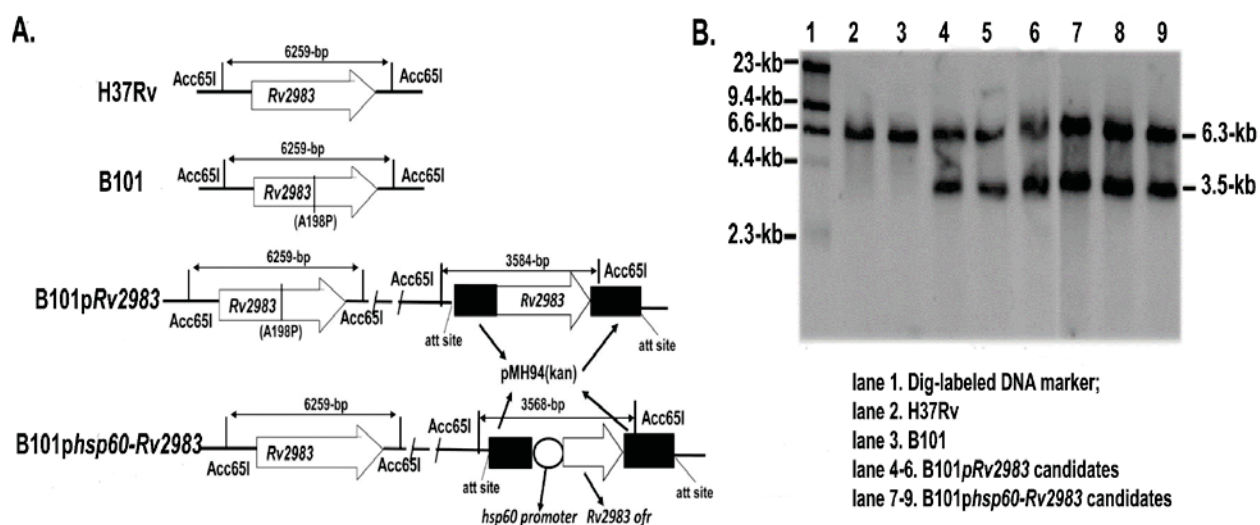| Mouse model	Isolate	Pretomanid treatment dose (mg/kg)	Pretomanid selection concentration (µg/ml)	Gene	Mutation	Agar-based MIC (µg/ml)	Broth-based MIC (µg/ml)
	H37Rv parent				wild-type	0.06	0.25
BALB/c	BA_002	0	0.25	*fgd1*	K9N	>32	
	BA_016	10	1	*fbiC*	L702R	>32	
	BA_101	300	1	*Rv2983*	A198P	32	
C3HeB/FeJ	KA_006	10	1	*fbiB*	del of T684	8	
	KA_058	100	1	*fbiA*	del of G47	>32	
	KA_091	300	1	*ddn*	D108 (IS6110 ins)	32	
	KA-016	10	0.25	*Rv2983*	Q114R		>32
	KA-026a	30	1	*fbiC*	IS6110 ins. in 85bp upstream of *fbiC*		>32

Figure S1. Complementation of B101 mutant with *Rv2983*. A. Schematic diagram of genomic DNA of *M. tuberculosis* strains after digestion with restriction enzyme Acc65I; B. Result of southern blot confirmed expected DNA fragments after Acc65I digestion using DIG-labeled *Rv2983* probe (H37Rv: 6.3 kb; Rv2983 mutant: 6.3 kb; complemented strains: 6.3 and 3.5 kb).
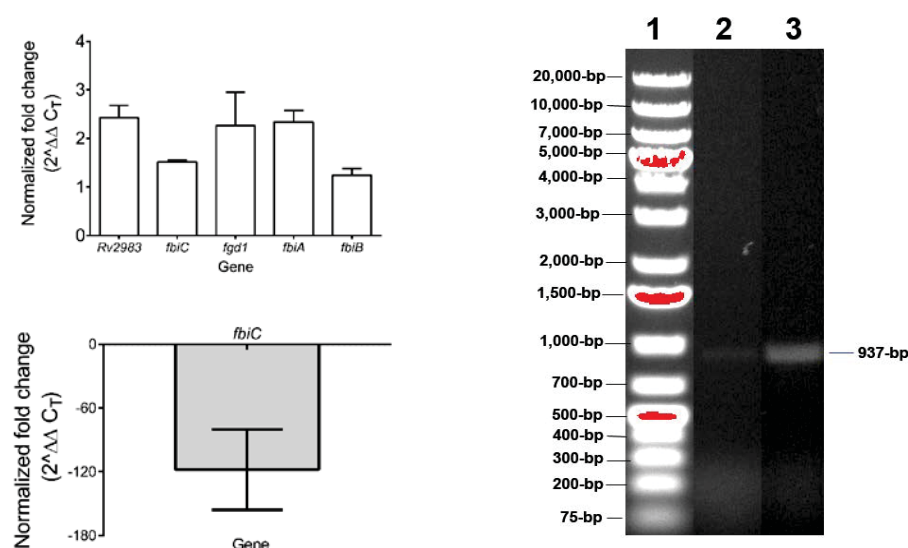
Figure S2. Expression of *Rv2983* and other genes involved in nitroimidazole activation. A. Expression of *Rv2983* and other genes involved in nitroimidazole activation is higher in the *Rv2983* mutant B101 relative to the wild-type H37Rv after 4 days of incubation in 7H9 broth; B. *fbiC* expression is dramatically lower in the *fbiC* mutant KA026 relative to the wild-type after 2 days of incubation in 7H9 broth; C. A faint band representing the 937-bp *fbiC* DNA fragment is evident in the sample from the KA026 mutant (lane 2) relative to that in H37Rv (lane 3). Lane 1 is the 1-kb DNA marker.
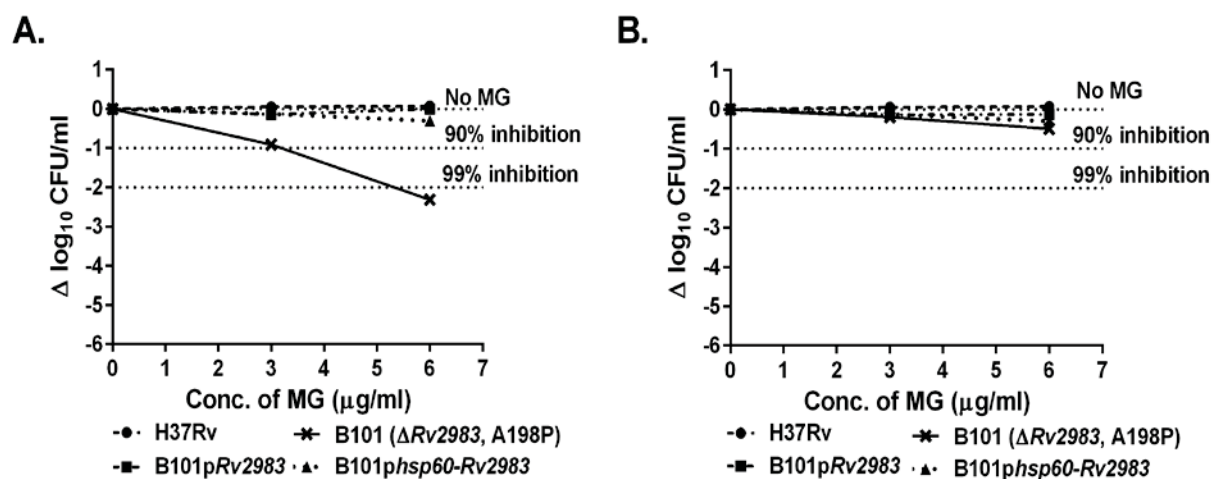
Figure S3. Complementation of the B101 mutant with wild-type *Rv2983* restores tolerance to MG. The proportional recovery of the mutant on 6 µg/ml of MG increases with the volume of culture plated and the duration of incubation: 28-day incubation of 500 µl (A) aliquots/plate; 35-day incubation of 500 µl (B) aliquots/plate.